



Pathogen lifestyle determines host genetic signature of quantitative disease resistance loci in oilseed rape (*Brassica napus*)

Catherine N. Jacott¹ · Henk-jan Schoonbeek¹ · Gurpinder Singh Sidhu² · Burkhard Steuernagel² · Rachel Kirby¹ · Xiaorong Zheng³ · Andreas von Tiedermann³ · Violetta K. Macioszek⁴ · Andrzej K. Kononowicz⁵ · Heather Fell⁶ · Bruce D. L. Fitt⁶ · Georgia K. Mitrousia^{6,7} · Henrik U. Stotz⁶ · Christopher J. Ridout¹ · Rachel Wells¹

Received: 25 November 2023 / Accepted: 30 January 2024 / Published online: 2 March 2024
© The Author(s) 2024

Abstract

Key message Using associative transcriptomics, our study identifies genes conferring resistance to four diverse fungal pathogens in crops, emphasizing key genetic determinants of multi-pathogen resistance.

Abstract Crops are affected by several pathogens, but these are rarely studied in parallel to identify common and unique genetic factors controlling diseases. Broad-spectrum quantitative disease resistance (QDR) is desirable for crop breeding as it confers resistance to several pathogen species. Here, we use associative transcriptomics (AT) to identify candidate gene loci associated with *Brassica napus* constitutive QDR to four contrasting fungal pathogens: *Alternaria brassicicola*, *Botrytis cinerea*, *Pyrenopeziza brassicae*, and *Verticillium longisporum*. We did not identify any shared loci associated with broad-spectrum QDR to fungal pathogens with contrasting lifestyles. Instead, we observed QDR dependent on the lifestyle of the pathogen—hemibiotrophic and necrotrophic pathogens had distinct QDR responses and associated loci, including some loci associated with early immunity. Furthermore, we identify a genomic deletion associated with resistance to *V. longisporum* and potentially broad-spectrum QDR. This is the first time AT has been used for several pathosystems simultaneously to identify host genetic loci involved in broad-spectrum QDR. We highlight constitutive expressed candidate loci for broad-spectrum QDR with no antagonistic effects on susceptibility to the other pathogens studies as candidates for crop breeding. In conclusion, this study represents an advancement in our understanding of broad-spectrum QDR in *B. napus* and is a significant resource for the scientific community.

Introduction

Crop-infecting fungi are responsible for approximately 20% of global crop losses annually (Fisher et al. 2018). Developing broad-spectrum resistance is vital for effective crop disease management, as it protects against several pathogen

Communicated by Lixi Jiang.

✉ Rachel Wells
rachel.wells@jic.ac.uk

¹ Crop Genetics Department, John Innes Centre, Norwich Research Park, Norwich NR4 7UH, UK

² Computational and Systems Biology Department, John Innes Centre, Norwich Research Park, Norwich NR4 7UH, UK

³ Department of Crop Sciences, Georg August University, 37077 Göttingen, Germany

⁴ Department of Biology and Plant Ecology, Faculty of Biology, University of Białystok, 15-245, Białystok, Poland

⁵ Department of Plant Ecophysiology, Faculty of Biology and Environmental Protection, University of Lodz, 90-237, Lodz, Poland

⁶ Centre for Agriculture, Food and Environmental Management Research, School of Life and Medical Sciences, University of Hertfordshire, Hatfield, Hertfordshire AL10 9AB, UK

⁷ Rothamsted Research, Harpenden, Hertfordshire AL5 2JQ, UK

species or most races or isolates of the same pathogen (Kou and Wang 2010). Despite this, plant interactions with different pathogens are rarely studied together in collaborative programs to identify common and unique genetic factors controlling the diseases.

Most research and breeding focus on “*R*” (resistance) gene-mediated qualitative resistance, often providing complete resistance to certain races of a pathogen (McDowell and Woffenden 2003). *R* gene-mediated resistance can be effective at controlling disease but often breaks down when pathogen effector genes mutate. In contrast, quantitative disease resistance (QDR)—also known as partial resistance—presents a continuous distribution of phenotypes from susceptible to resistant.

QDR has great potential for crop improvement due to its broad-spectrum and durable nature; however, it is not frequently targeted in breeding efforts due to a lack of insights into its underlying molecular determinants (Roux et al. 2014; Nelson et al. 2018). QDR is generally conferred by multiple genes, limiting the ability of pathogens to evolve resistance. QDR is likely broad-spectrum as it is often associated with constitutive features that affect the growth of diverse pathogens such as host plant morphology, basal defense, and signal transduction (Raman et al. 2020; Amas et al. 2022). Constitutive QDR may also function in combination with pathogen-specific resistance to prolong the effectiveness of *R* genes (Pilet-Nayel et al. 2017; Brun et al. 2010). Although few QDR genes have been cloned and functionally validated, reported mechanisms include enhanced cell wall synthesis (Wisser et al. 2005; Corwin et al. 2016), enhanced secondary metabolism (Benson et al. 2015), modified transport processes (Moore et al. 2015; Deppe et al. 2018), hormone synthesis, and transcriptional regulation (Qasim et al. 2020).

Identifying loci involved in broad-spectrum QDR to multiple pathogens is challenging. Different pathogens employ distinct infection and feeding strategies, including feeding on living host cells (biotrophy); killing plant cells to feed on their contents (necrotrophy); and keeping cells alive while establishing infection before switching to a necrotrophic mode (hemibiotrophy) (Kemen and Jones 2012). These diverse strategies necessitate differing plant defense mechanisms for effective resistance. For example, reactive oxygen species (ROS) production and cell death can provide resistance to biotrophic and hemibiotrophic pathogens (Jia et al. 2000; Vleeshouwers et al. 2000; Vetter et al. 2012). However, ROS accumulation and cell death can promote pathogenicity for some necrotrophic pathogens that use necrosis to facilitate their colonization (Tiedemann 1997; Govrin and Levine 2000; Lorang et al. 2007). Additionally, certain plant hormones such as salicylic acid (SA) and jasmonic acid (JA) exhibit opposing effects on resistance dependent on pathogen lifestyle (Navarro et al. 2008): The activation of the JA signaling provides resistance against

necrotrophic pathogens, but the activation of SA signaling protects against biotrophic and hemibiotrophic pathogens (Glazebrook 2005).

In addition, some broad-spectrum QDR mechanisms could relate to innate immunity based on the detection of shared pathogenic features irrespective of their lifestyle. For example, some quantitative trait loci (QTLs) implicated in QDR resemble cell surface pattern recognition receptors (PRRs) or receptor-like kinases (RLKs), akin to those in pathogen-associated molecular pattern (PAMP)-triggered immunity (PTI) (Nelson et al. 2018; Wisser et al. 2005; Lacombe et al. 2010; Schweizer and Stein 2011; Hurni et al. 2015; Schoonbeek et al. 2015). PRRs like CHITIN ELICITOR RECEPTOR-LIKE KINASE 1 (CERK1), FLAGELLIN SENSING 2 (FLS2), and EF-TU RECEPTOR (EFR) detect PAMPs such as chitin, flg22, and elf18, respectively (Miya et al. 2007; Gómez-Gómez and Boller 2000; Zipfel et al. 2006). Upon PAMP recognition, plants rapidly produce ROS like H₂O₂, followed by mitogen-activated protein kinase (MAPK) activation and defense gene induction. Measurement of ROS production by purified PAMPs has been used extensively in various laboratories to provide consistent and reliable PTI assessment and to study the relationship between PTI response and QDR (Vetter et al. 2012; Samira et al. 2020).

We aimed to identify broad-spectrum QDR loci in oilseed rape (*Brassica napus*) using a common panel of genotypes. *Brassica napus* is a major crop worldwide, producing edible oil, biodiesel, and animal feed protein. Disease susceptibility significantly impacts *B. napus* yields, so enhanced resistance is a major breeding objective. Employing associative transcriptomics (AT) (Harper et al. 2012; Havlickova et al. 2018), we previously identified single nucleotide polymorphism (SNP) and gene expression marker (GEM) candidate loci linked to *B. napus* QDR against *Pyrenopeziza brassicae* (Fell et al. 2023). The GEM analysis utilizes transcriptomic data representing a baseline pre-infection expression level—a foundation for investigating constitutive QDR. The AT pipeline has been successfully applied to diverse phenotypes including pathogen resistance, flowering time, and seed glucosinolate content (Harper et al. 2012; Woodhouse et al. 2021; Dakouri et al. 2021; Roy et al. 2021). However, to our knowledge, AT has never been used to research the similarities and differences between the loci underlying resistance to multiple pathogens.

Three hypotheses underlie our study. Firstly, using a diverse *B. napus* panel—comprising a range of crop types including winter, semi-winter, and spring oilseed rape, swede, and kale, resulting in 219k SNP variants across the genome—we hypothesized there would be variable pathogen resistance within the population due to the high level of genetic and morphological variation. This variation might correlate with constitutive defenses or early innate immunity

since PAMP recognition is conserved across pathogens. Therefore, our second hypothesis is that shared QDR loci may be associated with resistance to multiple pathogens, including those with contrasting lifestyles. Finally, given pathogens of different lifestyles utilize different mechanisms for their infection, our third hypothesis is that there would be some QDR loci dependent on the lifestyle of the pathogen. To test these hypotheses, we examined resistance to two necrotrophs, *Alternaria brassicicola* and *Botrytis cinerea*, and two hemibiotrophs, *P. brassicae* and *Verticillium longisporum*, within the diversity panel. We used AT to identify the associated loci that define the “host genetic signature” of QDR in *B. napus*. Additionally, we explored the presence of loci associated with both QDR and PTI (measured by the production of PAMP-induced ROS).

For the first time, we demonstrate that AT analyses from several pathogens can be combined to identify candidate loci for broad-spectrum QDR. We identify GEMs associated with either resistance or susceptibility dependent on the pathogen lifestyle. Additionally, we identify a potential deletion associated with resistance to *V. longisporum* and potentially broad-spectrum QDR. This study provides new insight into the commonalities underlying broad-spectrum QDR and provides a resource for further mechanistic exploration and improving broad-spectrum resistance to pathogens in *B. napus*.

Materials and methods

Pathogen infection assays

We selected a subset of the 193 *B. napus* genotypes for phenotyping, ensuring feasible pathology assays with ample replication across all participating laboratories. To mitigate environmental effects during seed production, all genotypes were cultivated under consistent environmental conditions before distribution to laboratories. Nevertheless, in some pathosystems, certain lines yielded unreliable data, leading to variable numbers of genotypes used for analyses.

Alternaria brassicicola

One-hundred-fifty-four *B. napus* accessions were grown in peat soil (pH 5.6–6.8) with 1/30 perlite, 16-h day/8-h night photoperiod under fluorescent light (Super TLD Philips 865, 100 $\mu\text{mol m}^{-2} \text{s}^{-1}$), 19 $^{\circ}\text{C} \pm 2^{\circ}\text{C}$, and approximately 70% relative humidity. The wild-type *A. brassicicola* strain (ATCC 96836) was cultured and previously described (Macioszek et al. 2018). A conidial suspension diluted to 3.5×10^5 conidia ml^{-1} in distilled water was applied in two 10- μl drops to the third leaf of five-week-old plants. Necrotic areas were measured in four complete block experimental

replicates, with one plant per genotype, at five days post-inoculation using WinDIAS_3 Imaging Analysis System (Delta-T Devices, UK).

Botrytis cinerea

We divided 190 *B. napus* accessions into four blocks for screening. Plants were grown in Levington F2 compost with 15% 4-mm grit in growth chambers for 6–7 weeks under TL-tubes with a near-sunlight spectrum of 100 $\mu\text{mol m}^{-2} \text{s}^{-1}$ with a photoperiod of 10 h. Temperatures were 20–22/18–20 $^{\circ}\text{C}$ day/night. *Botrytis cinerea* strain B05.10 (Schoonbeek et al. 2001) was grown as described previously (Stefanato et al. 2009) and used for inoculations as described (Lloyd et al. 2014). Spore suspensions (200 μl at 2.5×10^6 spores ml^{-1}) were spread on 1/10 PDA (2.5 g l^{-1} potato dextrose broth, 12 g l^{-1} agar), and after 24 h at 21 $^{\circ}\text{C}$, 4-mm agar plugs were used for *B. napus* inoculations of 22-mm leaf disks on 0.6% water agar. The lesion diameter was measured after 48 h at 21 $^{\circ}\text{C}$, 85–100% relative humidity, and low light (10–20 $\mu\text{mol m}^{-2} \text{s}^{-1}$). Reference genotypes, Tapidor and Ningyou 7, were included on each plate, and data were normalized to the mean of these reference lines before subsequent statistical analyses. Three full experimental replicates (divided into four blocks) within a randomized alpha block design were performed. From this, the two most reproducible experimental replicates, as determined by Pearson's coefficient, were selected for subsequent analyses. Sixteen replicates per genotype were performed per experimental replicate.

Pyrenopeziza brassicae

The *P. brassicae* methods and phenotype dataset used were the same as in our previous publication (Fell et al. 2022). The experiment comprised three complete experimental replicates, each divided into 10 blocks, following a randomized alpha block design. Within each experiment, five replicates were conducted for each genotype. Disease severity was scored on a scale of 1–6—with a score of 1 for no sporulation and 6 for the most sporulation—and was calculated for the 129 genotypes.

Verticillium longisporum

We divided 191 *B. napus* accessions into four blocks for screening. Four reference lines (Falcon, SEM, Zhongyou, Loras) were used for normalization. Each line had 20 plants for both mock and *V. longisporum* inoculation. The preparation of fungal inoculum and disease assessment were done as described previously (Zheng 2018; Zheng et al. 2019). Ten-day-old conidial suspension of *V. longisporum* isolate VL43 obtained from a diseased *B. napus* plant (Zeise et al. 2001)

was used for inoculation. Ten-day-old plants with unfolded cotyledons were inoculated with water or 1×10^6 CFU ml^{-1} spore suspension for 50 min. Plants were kept in a climate chamber with a 16-h photoperiod and 22 ± 2 °C temperature. Stem disease severity ranging from 1 (healthy) to 9 (dead) was assessed at 7, 14, 21, and 28 days post-inoculation. The area under the disease progress curve was calculated and normalized against reference lines.

ROS assays

One-hundred-ninety *B. napus* accessions were split into four groups and cultivated in Levington F2 compost with 15% 4-mm grit in growth chambers. A near-sunlight spectrum at around 100 $\mu\text{mol m}^{-2} \text{s}^{-1}$ and a 10-h photoperiod were maintained, with temperatures of 20–22 °C/18–20 °C day/night. ROS measurements employed a luminol/peroxidase-based assay. For each accession, two 4-mm-diameter leaf disks were taken from the second most recently expanded leaf of four individual plants. Two leaf disks per plant were taken, and the values obtained were averaged, resulting in four replicates per genotype. Leaf disks were incubated in 200- μl sterile water in a 96-well plate for 16–24 h in darkness. Subsequently, water was removed, and a solution was added containing 34-mg l-1 luminol, 20-mg l-1 horseradish peroxidase (HRP), and PAMP: either chitin (100 g l-1, NA-COS-Y, Yaizu Suisankagaku Industry CO., YSK, Yaizu, Japan); flg22 (QRLSTGSRINSAKDDAAGLQIA); or elf18 (SKEKFERTKPHVNVGTIG, both 10 mM, Peptron, <http://www.peptron.co.kr>). Luminescence was recorded over 40 min, and the total ROS response was quantified using area under the curve calculations. Reference genotypes, Tapidor and Ningyou 7, were included in each plate, and data were normalized to the mean of these reference lines before subsequent statistical analyses. Three full experimental replicates (divided into four blocks) within a randomized alpha block design were performed. From this, the two most reproducible experimental replicates, as determined by Pearson's coefficient, were selected for subsequent analyses.

Phenotypic data processing for association analysis

Each dataset (infection phenotypes for *A. brassicicola*, *B. cinerea*, *P. brassicae*, or *V. longisporum*, ROS measurements for chitin, flg22, or elf18) is available on Zenodo (<https://zenodo.org/records/10499917>). Statistical analysis was performed in R using the linear mixed model (lmer (trait ~ genotype_id) + (1|rep/block)) with genotype as a fixed effect and experimental replicate and block as nested random effects (with block being nested within replicate). Estimated marginal means were calculated for each *B. napus* genotype using emmeans Version 1.8.0 (R Core Team 2023). These mean values contributed by each collaborating laboratory for

each pathosystem were utilized as input for the AT pipeline. These data and standard errors are provided in Table S1. For combined data visualization, estimated marginal means were normalized to a 0–1 range. In pathogen datasets, the disease score is indicative of “susceptibility” to the pathogen. To represent “resistance” to the pathogen, the reciprocal of these values was calculated.

Associative transcriptomics

We used genotype (SNP) and expression level datasets (Havlickova et al. 2018) from York Knowledgebase (<http://yorkknowledgebase.info>) and refined to include only the lines used within this study. Functional genotypes were determined via 100-base mRNAseq for the third true leaf using the Illumina HiSeq 2000 platform. Sequence reads were mapped to the CDS gene model-based Brassica AC pan-transcriptome reference (He et al. 2015), which comprised 116,098 gene models for SNP scoring and read quantification; 219,454 SNPs with maternal allele frequencies greater than 5% were used for downstream analysis. Genome-wide Association (GWA) and GEM mapping were done using the R-based GWA and GEM Automation (GAGA) pipeline (Nichols 2022), which utilizes GAPIT Version 3 (Lipka et al. 2012; Wang 2021). GAGA was run using our recently updated population structure (Fell et al. 2023) and *B. napus* pan-transcriptome Version 11 (Havlickova et al 2018). For GWA analyses, generalized linear model (GLM), Bayesian-information and Linkage-disequilibrium Iteratively Nested Keyway (BLINK) (Huang et al. 2019), and Fixed and random model Circulating Probability Unification (FarmCPU) (Liu et al. 2016) models were compared using QQ plots to select the best-fitting model.

GEM association analyses were performed within the GAGA pipeline based on methodology by Harper et al. (2012). Associations were determined by linear regression using Reads per Kilobase of the transcript per Million mapped reads (RPKM) to predict a quantitative outcome of the trait value. Markers with an average expression below 0.5 RPKM were excluded prior to analysis resulting in 53,883 expression values for association analysis. The Pearson's coefficient was utilized to assess the correlation between expression and resistance phenotype for each GEM.

To determine the statistical significance threshold in GWA analysis, various methods that account for multiple testing have been proposed, including the Bonferroni correction and False Discovery Rate (FDR). Due to the prevalence of linked markers in modern GWA, the Bonferroni correction threshold can often have an inflated significance level, detecting only strong, major gene effects as significant. To address this, we utilized the FDR to manage the expected proportion of false positives among significant associations. FDR values for both GEM and GWA were determined using

the q value R package (Storey 2011). Bonferroni thresholds for GWA and GEM are 6.64 and 6.03- $\text{Log}_{10}P$, respectively, ($P < 0.05$) and 6.34 and 5.73 $-\text{Log}_{10}P$ ($P < 0.1$).

Linkage disequilibrium (LD) varies based on chromosome position and selection level. To ascertain the LD at the A09 locus associated with *V. longisporum* resistance, we calculated the mean pairwise R^2 between this marker and all others on the chromosome using the TASSEL Version 5.0 site by all analysis options (Bradbury et al. 2007). Markers were deemed in LD when $R^2 > 0.2$.

Interpretation of data post-AT

To determine query coverage (proportion of query sequence aligning with reference sequence) for the genomic region in linkage disequilibrium with the most significant SNP marker associated with *V. longisporum* resistance, we conducted a command line BLAST analysis against the *B. napus* pan-transcriptome. The analysis was performed for genotypes included in our study with published reference genomes: Quinta, Tapidor, Westar, and Zhongshuang 11 (Song et al. 2020).

We identified potential *Arabidopsis thaliana* orthologs of *B. napus* genes using BLASTN analysis against the *A. thaliana* transcriptome (TAIR Version 10), selecting the best hit based on e value. Hypergeometric probability was used for to determine whether the number of overlapping GEMs observed was greater than that expected by chance as detailed by Kim et al. (2001).

We conducted weighted gene co-expression analysis (WGCNA) using the R-based WGCNA library (v 1.72) (Langfelder and Horvath 2008). Lowly expressed genes with 0 RPKM value in half of the samples were removed, and the rest of the data were used to perform a signed WGCNA analysis to detect modules of genes using the `blockwiseModules()` function. A soft threshold power of 6 was selected based on minimum mean connectivity using the `pickSoft-Threshold()` function within the WGCNA package. Correlation and P values with phenotypic trait data were calculated using the “`Cor()`” and “`CorPvalueStudent()`” functions. Gene Ontology (GO) enrichment analysis ($\text{FDR} < 0.05$) was conducted using a Fisher’s exact test for GEMs within WGCNA modules.

Results

QDR to *A. brassicicola*, *B. cinerea*, *P. brassicae*, and *V. longisporum* is present in the *B. napus* diversity panel

Given the extensive genetic diversity in our *B. napus* panel, we hypothesized that QDR to *A. brassicicola*, *B. cinerea*,

P. brassicae, and *V. longisporum* would be present. We did pathogenicity assays and found that the *B. napus* genotypes demonstrated varying levels of resistance to the pathogens, confirming the presence of QDR in the panel (Fig. 1a, Table S1).

We hypothesized that if broad-spectrum QDR was present, there would be a positive correlation between phenotypic responses to pathogens. We initially examined disease resistance in four *B. napus* genotypes with published reference genomes: Quinta, Tapidor, Westar, and Zhongshuang 11. Quinta showed low resistance to both hemibiotrophic pathogens, while Zhongshuang 11 displayed high resistance to both necrotrophic pathogens (Fig. 1a). However, the ranking of these reference genotypes within the diversity panel varied. To explore phenotypic correlations between responses to pathogens across the entire *B. napus* panel, we generated a correlation matrix for pairwise fungal pathogen comparisons using the respective phenotypic resistance scores for each genotype (Fig. 1b). There was a positive correlation between resistance to necrotrophic pathogens *A. brassicicola* and *B. cinerea*. Conversely, negative correlations emerged between resistance to different pathogen lifestyles; for example, hemibiotrophic *V. longisporum* showed negative correlations with necrotrophic pathogens *A. brassicicola* and *B. cinerea*.

GEMs are associated with resistance to pathogens of the same lifestyle

To identify QDR loci, we performed GWA analysis on our datasets from the four fungal pathogens. Minor GWA association peaks could be observed ($-\text{Log}_{10}P > 5$); however, we did not identify any significant marker associations with resistance to any of the pathogens, using either a Bonferroni threshold of $P = 0.1$ or a False Discovery Rate (FDR) of 0.05. All association data provided are in Table S2. We performed GEM analyses using the transcriptomes of the *B. napus* genotypes to associate resistance with the expression of all gene models (Table S3). Numerous GEMs showed significant associations with fungal pathogen resistance ($\text{FDR} < 0.05$), and these were distributed evenly across the *B. napus* genome (Fig. 1c): 2129 GEMs for *A. brassicicola*, 370 for *B. cinerea*, 659 for *P. brassicae*, and 3222 for *V. longisporum*. We classified GEMs based on their positive or negative correlation with resistance or susceptibility, naming them “resistance GEMs” or “susceptibility GEMs,” respectively (Table 1).

We hypothesized that there might be shared QDR GEMs associated with all four fungal pathogens given that some early innate defense mechanisms such as PAMP recognition are conserved across most pathogens. To investigate this, we compared the lists of resistance and susceptibility GEMs across the fungal pathogens (Fig. 1d). While necrotrophic

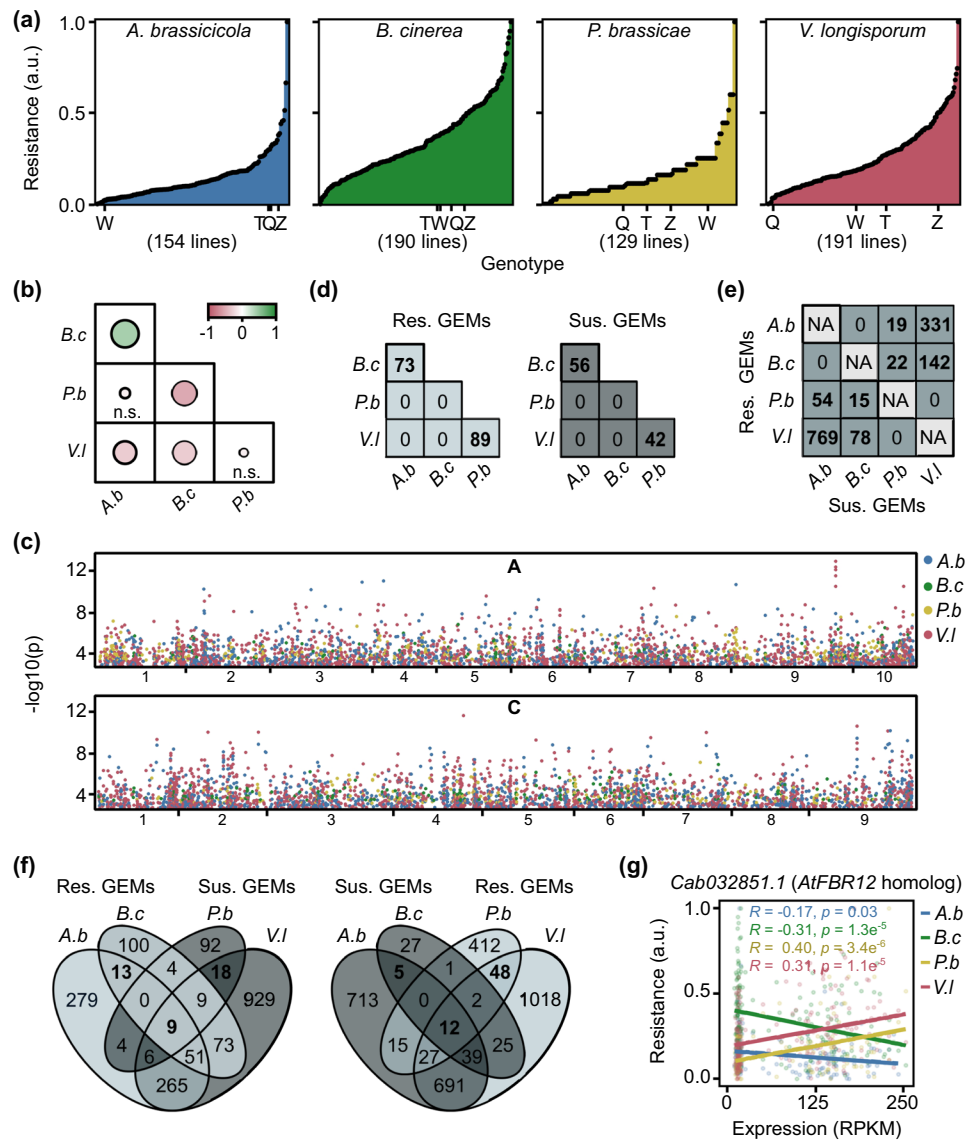


Fig. 1 *Brassica napus* genotypes have common GEMs associated with resistance pathogens of the same lifestyle. **a** *Brassica napus* disease resistance to fungal pathogens is quantitative. Resistance phenotype (arbitrary units (a.u.)) of different *B. napus* genotypes to *Alternaria brassicicola* (*A.b*), *Botrytis cinerea* (*B.c*), *Pyrenopeziza brassicae* (*P.b*), or *Verticillium longisporum* (*V.l*). Arbitrary units signify resistance values obtained through the reciprocal of disease susceptibility scores, derived from estimated marginal means and normalized to a 0–1 range for comparative data visualization. The total number of genotypes used for each pathogen assay and the position of reference genotypes Quinta (Q), Tapidor (T), Westar (W), and Zhongshuang 11 (Z) are indicated. **b** Correlation between the resistance phenotype of *B. napus* lines to the fungal pathogens. Positive correlations (green), negative correlations (red), and no correlation (n.s.); strengths of correlation (sizes of circles) are indicated between

pairwise comparisons of resistance responses. **c** Manhattan plot of *B. napus* genome showing marker-trait association of statistically significant GEMs for resistance to each fungal pathogen. The x-axis indicates GEM location along the chromosome; the y-axis indicates the $-\log_{10}(p)$ (*P* value). **d** The numbers of resistance and susceptibility gene expression markers (GEMs) shared between pairwise comparisons of pathogens. **e** The numbers of GEMs associated with resistance to one pathogen and susceptibility to another pathogen. **f** Venn diagrams showing the overlap between *A.b* and *B.c* susceptibility GEMs and *P.b* and *V.l* resistance GEMs (right) and the overlap between *A.b* and *B.c* resistance GEMs and *P.b* and *V.l* susceptibility GEMs (left). **g** Linear regression analysis of gene expression (RPKM) of *Cab032851.1* relative to resistance to fungal pathogens (arbitrary units (a.u.), normalized values between zero and one)

pathogens (*A. brassicicola* and *B. cinerea*) had shared GEMs, as did hemibiotrophic pathogens (*P. brassicae* and *V. longisporum*), there were no common GEMs between necrotrophic and hemibiotrophic pathogens. Consequently,

there were no shared GEMs associated with broad-spectrum resistance spanning pathogens with differing lifestyles.

Given the existence of shared QDR GEMs associated with pathogens of the same lifestyle and that pathogens with

Table 1 The number of gene expression markers (GEMs) associated with resistance to *Brassica napus* different fungal pathogens. *Alternaria brassicicola*, *Botrytis cinerea*, *Pyrenopeziza brassicae*, and *Verticillium longisporum* fungal pathogens are indicated. The total numbers of GEMs, GEMs with expression positively correlated with resistance (*R*, resistance) and negatively correlated with resistance (*S*, susceptibility) are indicated

Pathogen	Number of GEMs (FDR < 0.05)		
	Total	<i>R</i>	<i>S</i>
<i>A. brassicicola</i>	2129	627	1502
<i>B. cinerea</i>	370	259	111
<i>P. brassicae</i>	659	517	142
<i>V. longisporum</i>	3222	1862	1360

similar lifestyles have similarities related to their infection, feeding strategies, and plant processes required for defense, we conducted overrepresentation analyses to compare the number of shared QDR GEMs between pathogens of the same lifestyle against what would be expected by chance (Plaisier et al. 2010). There was significant overrepresentation in the number of shared GEMs between necrotrophic pathogens *A. brassicicola* and *B. cinerea* (73 resistance GEMs and 56 susceptibility GEMs), as well as between hemibiotrophic pathogens *P. brassicae* and *V. longisporum* (89 resistance GEMs and 42 susceptibility GEMs) (Fig. 1d, Tables S4, S5).

GEMs are associated antagonistically with resistance to pathogens of different lifestyles

Hemibiotrophic and necrotrophic pathogens employ distinct plant mechanisms for their infection, with certain genes that confer resistance to hemibiotrophic pathogens leading to susceptibility against necrotrophic pathogens (Lorang et al. 2007). Thus, we hypothesized the presence of QDR GEMs with antagonistic associations based on pathogen lifestyle. To explore this, we compared resistance GEMs with susceptibility GEMs for each combination of fungal pathogens (Fig. 1e). As anticipated, there were no GEMs with antagonistic effects for pairs of either necrotrophic or hemibiotrophic pathogens. However, intriguingly, we observed an overrepresentation of GEMs with antagonistic resistance associations between necrotrophic and hemibiotrophic pathogens. For instance, 1100 (769 + 331) GEMs with opposite resistance associations were linked to *A. brassicicola* and *V. longisporum* (Tables S4, S5).

Broad-spectrum resistance GEMs with no antagonistic effects on susceptibility to other pathogens hold promise for crop breeding. To identify such candidates, we compared necrotrophic pathogen susceptibility GEMs to hemibiotrophic pathogen resistance GEMs. Similarly, we compared necrotrophic pathogen resistance GEMs to hemibiotrophic

pathogen susceptibility GEMs (Fig. 1f, Table S4). Thirteen GEMs were associated with resistance to both *A. brassicicola* and *B. cinerea* with no associations with susceptibility to *P. brassicae* and *V. longisporum* (Table 2). Forty-eight GEMs were associated with resistance to both *P. brassicae* and *V. longisporum* with no associations with susceptibility to *A. brassicicola* and *B. cinerea* (Table 3). Notably, four GEMs homologous to *A. thaliana ACIP1* were associated with resistance to both hemibiotrophic pathogens and no antagonistic associations with susceptibility to the necrotrophic pathogens.

Interestingly, there was a significant overrepresentation of GEMs associated with susceptibility or resistance to both necrotrophic pathogens, but with opposing associations to both hemibiotrophic pathogens: 21 GEMs (9 + 12) (Table 4, S6). Notably, the expression of *Cab032821.1*, the homolog of *A. thaliana Fumonisin B1-resistant 12, FBR12*, was associated with resistance to both hemibiotrophic pathogens but susceptibility to both necrotrophic pathogens (Fig. 1g), as was the *Bo8g081460.1*, the homolog of an *A. thaliana disease resistance nucleotide-binding leucine-rich repeat (NBS-LRR)* protein (Table 4).

We conducted weighted gene co-expression analysis (WGCNA) (Langfelder and Horvath 2008) to explore the co-expression patterns of GEMs in our study. Several GEMs exhibited co-expression patterns across the *B. napus* population and were organized into co-expression modules. These modules were then assessed for their association with resistance to each pathogen (Table S6). Notably, significantly correlated modules included 22 modules (containing a total of 1075 GEMs) for resistance to *A. brassicicola*, 18 modules (containing 299 GEMs) for resistance to *B. cinerea*, 34 modules (containing 575 GEMs) for resistance to *P. brassicae*, and 26 modules (containing 2075 GEMs) for resistance to *V. longisporum*. Interestingly, modules correlated with resistance to necrotrophic pathogens displayed susceptibility to hemibiotrophic pathogens, and vice versa, consistent with the findings from our individual GEM results.

To gain further insights, we performed GO enrichment analysis on the putative *A. thaliana* orthologs of resistance and susceptibility GEMs within each module. Particularly noteworthy was a module linked to susceptibility to necrotrophic pathogens and resistance to hemibiotrophic pathogens, enriched in genes associated with photosynthesis, suggesting that photosynthesis-related processes might exert contrasting effects on resistance based on the pathogen's lifestyle. We examined whether there were any GEMs related to known pathogen-dependent pathways, specifically SA or JA signaling. We first used gene ontology to search for SA- or JA-related GEMs in our whole expression dataset (53,883 markers). No GEMs were linked to SA signaling, and markers associated with JA signaling were not enriched in our GEM analysis or WGCNA modules. This is likely because

Table 2 Broad-spectrum GEMs associated with resistance (*R*) or susceptibility (*S*) to necrotrophic fungi (necro.) with no associations with hemibiotrophic fungi (hemi.). Hemibiotrophic pathogens include *Pyrenopeziza brassicae* and *Verticillium longisporum* and necrotrophic

pathogens include *Alternaria brassicicola* and *Botrytis cinerea*. The putative *Arabidopsis thaliana* (*At*) orthologs and gene ID are indicated

GEM	Necro.	Hemi.	<i>At</i> ortholog	Gene name	Protein class
<i>Cab019641.1</i>	<i>R</i>	–	–	–	–
<i>Cab029666.1</i>	<i>R</i>	–	<i>AT1G04980.1</i>	<i>PDII0</i> ; Protein disulfide-isomerase like 2–2	Chaperone
<i>Cab006731.1</i>	<i>R</i>	–	–	–	–
<i>Cab023848.3</i>	<i>R</i>	–	<i>AT3G13772.1</i>	<i>TMN7</i> ; Transmembrane 9 superfamily member 7	Transporter
<i>Bo6rg071140.1</i>	<i>R</i>	–	<i>AT3G56460.1</i>	<i>GroES-like zinc-binding alcohol dehydrogenase family protein</i>	Oxidoreductase
<i>Cab006719.1</i>	<i>R</i>	–	<i>AT5G24630.5</i>	<i>BIN4</i> ; Brassinosteroid insensitive 4	DNA-binding
<i>Bo3g028280.1</i>	<i>R</i>	–	<i>AT4G38220.2</i>	<i>AQI</i> ; Aquaporin interactor, <i>N</i> -acyl- <i>L</i> -amino-acid amidohydrolase	–
<i>Bo9g183340.1</i>	<i>R</i>	–	<i>AT5G02820.1</i>	<i>BIN5</i> ; Brassinosteroid insensitive 5, DNA topoisomerase 6 subunit A	Endodeoxyribonuclease
<i>Bo3g004890.1</i>	<i>R</i>	–	<i>AT5G08380.1</i>	<i>AGAL1</i> ; Alpha-galactosidase 1	Galactosidase
<i>Cab010087.2</i>	<i>R</i>	–	–	–	–
<i>Cab023861.2</i>	<i>R</i>	–	<i>AT1G72730.1</i>	<i>Eukaryotic initiation factor 4A-3</i>	RNA helicase
<i>BnaC03g41840D</i>	<i>R</i>	–	–	–	–
<i>Bo1g017790.1</i>	<i>R</i>	–	<i>AT4G17720.1</i>	<i>BPL1</i> ; Putative RRM-containing protein	RNA splicing factor
<i>Cab007046.1</i>	<i>S</i>	–	<i>AT5G48590.1</i>	–	–
<i>Bo5g132170.1</i>	<i>S</i>	–	<i>AT3G13740.1</i>	<i>RNC4</i> ; RNase III-like enzyme	–
<i>Cab029917.1</i>	<i>S</i>	–	<i>AT1G01090.1</i>	<i>PDH-E1 ALPHA</i> ; Pyruvate dehydrogenase E1 subunit alpha-3	Dehydrogenase
<i>Bo3g040470.1</i>	<i>S</i>	–	<i>AT2G27510.1</i>	<i>FD3</i> ; Ferredoxin-3	Reductase
<i>Bo5g132390.1</i>	<i>S</i>	–	<i>AT3G13550.1</i>	<i>COP10</i> ; Constitutive photomorphogenesis protein 10	Ubiquitin-protein ligase

these genes are usually activated in response to pathogens rather than being constitutively expressed at the represented three-leaf stage in our expression data.

GEMs associated with both PTI and QDR are dependent on pathogen lifestyle

We had originally hypothesized the presence of shared QDR loci associated with resistance to multiple pathogens with contrasting lifestyles possibly linked to early innate immunity due to the conserved nature of PAMP recognition. However, our comparisons of GEMs (Fig. 1d) revealed no shared GEMs between all four pathogens. Nevertheless, previous studies have linked PTI genes to QDR (Nelson et al. 2017; Wissner et al. 2005; Schweiser and Stein 2011; Hurni et al. 2015). Thus, we proceeded to investigate whether any of our pathogen resistance QDR loci were related to PTI.

The *B. napus* genotypes demonstrated varying levels of PAMP-induced ROS production with all three PAMPs, suggesting quantitative traits (Figs. 2a, S1a). Reference lines (Quinta, Tapidor, Westar, and Zhongshuang 11) had comparable rankings for flg22 and elf18 ROS responses within the panel, and our correlation matrix indicated that the *B. napus* genotypes exhibited similar rankings of responses across all three PAMPs (Fig. S2b). Minor GWA association peaks could be observed ($-\text{Log}_{10}P > 5$), with a single marker (*Cab031873.1:1209:C*) significantly associated with

flg22-induced ROS production at a Bonferroni threshold of $P = 0.1$. No significantly associated markers were observed at an FDR of 0.05. All marker associations are detailed in Table S2. We identified 184, 286, and 3251 GEMs associated with chitin-, flg22-, and elf18-induced ROS responses, respectively (Table S3); however, no GEMs corresponded to PRRs. There was a significant overlap between GEMs associated with the different PAMP responses. For example, out of the 184 chitin-induced ROS GEMs, 31% were shared with the flg22 response, 54% with the elf18 response, and 21% with both flg22 and elf18 responses (Table S7, Fig. S1c). These data suggest that response to PAMPs has some general genetic control and some PAMP-dependent distinct elements.

Since chitin is a fungal PAMP and our study centers on fungal pathogens, we concentrated our following investigations on the overlap between chitin-associated and QDR-associated loci. Chitin-induced ROS response did not correlate with QDR to fungal pathogens (Fig. 2b), and only a small fraction (less than 1%) of QDR GEMs for each pathogen were linked to chitin-induced ROS response (Table S7). Notably, there was minimal overlap between GEMs associated with chitin-induced ROS response and QDR to necrotrophic pathogens, and a slight overlap with QDR to hemibiotrophic pathogens (Table S5). This suggests that most QDR loci are independent of early PAMP-induced ROS response (Fig. 2c).

Table 3 Broad-spectrum GEMs associated with resistance (*R*) or susceptibility (*S*) to hemibiotrophic fungi (hemi.) with no associations to necrotrophic fungi (necro.). Hemibiotrophic pathogens include *Pyrenopeziza brassicae* and *Verticillium longisporum* and necrotrophic pathogens include *Alternaria brassicicola* and *Botrytis cinerea*. The putative *Arabidopsis thaliana* (*At*) orthologs and gene ID are indicated. GEMs corresponding to *A. thaliana* AT3G09980.1 are highlighted in bold

GEM	Necro.	Hemi.	At ortholog	Gene name	Protein class
<i>BnaC09g43580D</i>	–	<i>R</i>	–	–	–
<i>Cab025354.2</i>	–	<i>R</i>	<i>AT2G45580.1</i>	<i>CYP76C3</i> ; Cytochrome P450, family 76, subfamily C, polypeptide 3	–
<i>Bo4g182630.1</i>	–	<i>R</i>	<i>AT2G34470.1</i>	<i>UREG</i> ; Urease accessory protein G	–
<i>Bo5g058580.1</i>	–	<i>R</i>	<i>AT3G09980.1</i>	<i>ACIPI</i> ; Acetylated interacting protein 1	–
<i>Bo4g183100.1</i>	–	<i>R</i>	<i>AT2G35190.1</i>	<i>NPSN11</i> ; Novel plant SNARE 11	SNARE protein
<i>Bo2g095510.1</i>	–	<i>R</i>	<i>AT1G80930.1</i>	Pre-mRNA splicing factor CWC22 homolog	RNA processing factor
<i>Bo9g176470.1</i>	–	<i>R</i>	<i>AT5G06250.2</i>	<i>NGAL3</i> ; <i>NGATHA</i> -like protein 3, B3 domain-containing protein	Transcription factor
<i>BnaC03g64760D</i>	–	<i>R</i>	<i>AT3G09980.1</i>	<i>ACIPI</i> ; Acetylated interacting protein 1	–
<i>Cab042580.1</i>	–	<i>R</i>	<i>AT4G02710.1</i>	<i>NET1C</i> ; Protein NETWORKED 1C, Ki-se interacting (<i>KIP1</i> -like)	–
<i>Bo4g045470.1</i>	–	<i>R</i>	<i>AT2G32860.1</i>	<i>BGLU33</i> ; Beta glucosidase 33	–
<i>Bo4g182440.1</i>	–	<i>R</i>	<i>AT2G34250.2</i>	<i>SecY/Sec61-alpha</i> family member protein	Transporter
<i>Cab042707.1</i>	–	<i>R</i>	<i>AT5G51120.1</i>	<i>PAMN1</i> ; Polyadenylate-binding protein 1 homolog	Translation initiation factor
<i>Cab037277.2</i>	–	<i>R</i>	<i>AT3G22550.1</i>	<i>FLZ8</i> ; FCS-Like Zinc finger 8	–
<i>Bo4g183310.1</i>	–	<i>R</i>	<i>AT2G35510.1</i>	<i>SRO1</i> , similar to RCD 1, I-active poly [ADP-ribose] polymerase	–
<i>Cab025625.4</i>	–	<i>R</i>	–	–	–
<i>Bo6rg103690.1</i>	–	<i>R</i>	<i>AT1G67280.2</i>	<i>GLYI6</i> ; Lactoylglutathione lyase	Lyase
<i>Bo4g182680.1</i>	–	<i>R</i>	–	–	–
<i>Bo2g095560.1</i>	–	<i>R</i>	–	–	–
<i>Cab029121.1</i>	–	<i>R</i>	<i>AT2G26250.1</i>	<i>KCS10</i> ; 3-Ketoacyl-CoA synthase 10	–
<i>Bo5g137820.1</i>	–	<i>R</i>	<i>AT3G09980.1</i>	<i>ACIPI</i> ; Acetylated interacting protein 1	–
<i>Bo4g194830.1</i>	–	<i>R</i>	<i>AT2G44120.1</i>	60S ribosomal protein L7-3	Ribosomal protein
<i>Cab013800.1</i>	–	<i>R</i>	<i>AT1G16445.1</i>	<i>S-adenosyl-L-methionine-dependent methyltransferases superfamily</i>	Methyltransferase
<i>Bo2g095550.1</i>	–	<i>R</i>	–	–	–
<i>Bo4g182550.1</i>	–	<i>R</i>	<i>AT2G34410.2</i>	<i>RWA3</i> ; Reduced wall acetylation 3 homolog	–
<i>Bo4g182960.1</i>	–	<i>R</i>	<i>AT2G34840.1</i>	<i>epsilon2-COP</i> ; Coatomer subunit epsilon-2	Vesicle coat protein
<i>Bo1g051850.1</i>	–	<i>R</i>	<i>AT2G31290.2</i>	Ubiquitin carboxyl-terminal hydrolase family protein	–
<i>BnaC06g39270D</i>	–	<i>R</i>	–	–	–
<i>Bo1g003050.1</i>	–	<i>R</i>	<i>AT4G40000.1</i>	<i>TRM4A</i> ; <i>S-adenosyl-L-methionine-dependent methyltransferase</i>	R-methyltransferase
<i>Bo4g023900.1</i>	–	<i>R</i>	<i>AT2G44620.1</i>	Acyl carrier protein 1, mitochondrial	–
<i>Cab002494.2</i>	–	<i>R</i>	<i>AT2G30320.1</i>	–	–
<i>Cab007584.1</i>	–	<i>R</i>	<i>AT5G05800.2</i>	<i>L10-interacting MYB domain-containing protein</i>	–
<i>BnaC04g02850D</i>	–	<i>R</i>	<i>AT3G09980.1</i>	<i>ACIPI</i> ; Acetylated interacting protein 1	–
<i>BnaC05g07480D</i>	–	<i>R</i>	–	–	–
<i>Bo5g003800.1</i>	–	<i>R</i>	<i>AT1G03365.1</i>	Putative E3 ubiquitin-protein ligase RF4	–
<i>Cab042031.1</i>	–	<i>R</i>	–	–	–
<i>Bo4g183270.1</i>	–	<i>R</i>	–	–	–
<i>Bo4g183070.1</i>	–	<i>R</i>	<i>AT2G35050.1</i>	Kinase superfamily domain-containing protein	Non-receptor ser/thr kinase
<i>Bo4g182310.1</i>	–	<i>R</i>	<i>AT2G33860.1</i>	<i>ARF3/ETT</i> ; Auxin response factor 3/ETTIN	–
<i>Cab019919.4</i>	–	<i>R</i>	<i>AT4G31040.1</i>	<i>DLDG1</i> ; Chloroplast envelope membrane protein	–
<i>Bo6rg003510.1</i>	–	<i>R</i>	<i>AT3G18524.1</i>	<i>MSH2</i> ; DNA mismatch repair protein	D-metabolism protein
<i>Cab019786.1</i>	–	<i>R</i>	<i>AT4G29530.1</i>	<i>THMPASE1</i> ; Thiamine phosphate phosphatase-like protein	Phosphatase
<i>Bo4g182420.1</i>	–	<i>R</i>	<i>AT3G18430.2</i>	Calcium-binding EF-hand family protein	–

Table 3 (continued)

GEM	Necro.	Hemi.	At ortholog	Gene name	Protein class
<i>Bo6rg003540.1</i>	–	R	<i>AT1G44790.1</i>	<i>Gamma-glutamylcyclotransferase 2–3</i>	–
<i>Cab007776.1</i>	–	R	<i>AT5G11710.1</i>	<i>EPS1; Clathrin interactor EPSIN 1</i>	Membrane trafficking
<i>Bo4g183130.1</i>	–	R	<i>AT2G35230.1</i>	<i>IKU1; Protein HAIKU1</i>	–
<i>Bo4g143960.1</i>	–	R	<i>AT5G37890.1</i>	<i>SI-L7; E3 ubiquitin-protein ligase SI-like 7</i>	Ubiquitin-protein ligase
<i>Cab007778.1</i>	–	R	–	–	–
<i>Bo6rg003520.1</i>	–	R	<i>AT1G44770.1</i>	<i>Elongation factor</i>	–
<i>Cab019945.1</i>	–	S	–	–	–
<i>Cab044891.1</i>	–	S	–	–	–
<i>BnaA08g28590D</i>	–	S	–	–	–
<i>Bo6rg033210.1</i>	–	S	<i>AT1G55090.1</i>	<i>Glutamine-dependent -D(+) synthetase</i>	Ligase
<i>BnaC08g18360D</i>	–	S	–	–	–
<i>Bo2g007540.1</i>	–	S	<i>AT5G07210.1</i>	<i>ARR21; Putative two-component response regulator 21</i>	Transcription factor
<i>BnaA01g02330D</i>	–	S	–	–	–
<i>Cab002672.1</i>	–	S	<i>AT2G33810.1</i>	<i>SPL3; Squamosa promoter binding protein-like 3</i>	DNA-binding
<i>Cab013528.1</i>	–	S	–	–	–
<i>Cab034921.1</i>	–	S	<i>AT2G38540.1</i>	<i>LP1; Non-specific lipid-transfer protein 1</i>	–
<i>Cab020282.2</i>	–	S	–	–	–
<i>Bo7g095690.1</i>	–	S	<i>AT5G25830.1</i>	<i>GATA12; GATA transcription factor 12</i>	Transcription factor
<i>BnaC08g15170D</i>	–	S	–	–	–
<i>Cab037036.1</i>	–	S	–	–	–
<i>Cab034089.1</i>	–	S	–	–	–
<i>Bo8g087140.1</i>	–	S	<i>AT3G54890.1</i>	<i>LHCA1; Light-harvesting complex gene 1</i>	–
<i>Bo6rg098720.1</i>	–	S	<i>AT1G67700.1</i>	<i>HHL1; Hypersensitive to high light 1</i>	–
<i>Bo5g152840.1</i>	–	S	<i>AT3G02150.2</i>	<i>PTF1; Plastid transcription factor 1</i>	Transcription factor

Given that ROS accumulation can influence susceptibility to certain necrotrophic pathogens and our previous observation of QDR GEMs with lifestyle-dependent antagonistic associations, we investigated whether loci linked to chitin-induced ROS production might be associated with resistance against hemibiotrophic pathogens but susceptibility to necrotrophic pathogens. Of the 184 GEMs that were associated with chitin-induced ROS, 142 were positively associated, i.e., increased gene expression was associated with the increased magnitude of chitin-induced ROS response. Remarkably, all positively associated chitin-induced ROS GEMs that coincided with QDR GEMs were exclusively associated with resistance to hemibiotrophic pathogens and susceptibility to necrotrophic pathogens (Fig. 2d, Table 5). These included *BnaC04g02850D*, a homolog of *A. thaliana ACIP1* (also associated with *flg22* and *elf18* responses), and *Cab022449.1*, a homolog of *A. thaliana Aldehyde dehydrogenase 3H1 (ALDH3H1)* (Fig. 2e, Table S4). Likewise, among the 42 GEMs exhibiting negative correlations with chitin-induced ROS response, those overlapping with QDR were associated with resistance against necrotrophic pathogens and susceptibility to hemibiotrophic pathogens. WGCNA analysis revealed that GEMs linked to chitin-induced ROS were grouped into 19 modules (comprising

135 GEMs) (Table S6). In line with our individual GEM results, modules positively associated with chitin-induced ROS production were associated with resistance to hemibiotrophic pathogens and susceptibility to necrotrophic pathogens, including the module enriched in GEMs related to photosynthesis regulation.

A 0.51 MB deletion on chromosome A09 is associated with *V. longisporum* resistance and potentially broad-spectrum QDR

The genomic distribution of GEMs (Fig. 1C) highlighted a notable peak of five highly significant GEMs associated with *V. longisporum* resistance on chromosome A09 (*Cab013522.1*, *Cab013524.1*, *Cab013523.1*, *Cab013526.1*, and *Cab013517.1*). Notably, *Cab013522.1*, *Cab013524.1*, and *Cab013526.1* were also linked to *P. brassicae* resistance, while *Cab013522.1*, *Cab013523.1*, *Cab013524.1*, and *Cab013526.1* were associated with susceptibility to *A. brassicicola* (Table S3). This clustering suggests a potential region of interest for broad-spectrum QDR. Compellingly, this region of chromosome A09 also corresponded to a minor association ($P = 5.14e^{-07}$, FDR = 0.11) from the *V. longisporum* resistance GWA analysis (Fig. 3a).

Table 4 Broad-spectrum GEMs associated with resistance (*R*) or susceptibility (*S*) to hemibiotrophic fungi (hemi.) with antagonistic associations to necrotrophic fungi (necro.). Hemibiotrophic pathogens include *Pyrenopeziza brassicae* and *Verticillium longisporum* andnecrotrophic pathogens include *Alternaria brassicicola* and *Botrytis cinerea*. The putative *Arabidopsis thaliana* (*At*) orthologs, gene ID, and protein class are indicated

GEM	Necro.	Hemi.	<i>At</i> ortholog	Gene name	Protein class
<i>BnaA10g08980D</i>	<i>R</i>	<i>S</i>	AT2G34470.2	UREG; Urease accessory protein G	–
<i>Bo2g101920.1</i>	<i>R</i>	<i>S</i>	AT3G10020.1	HUP26; Hypoxia unknown protein 26	–
<i>Cab002732.1</i>	<i>R</i>	<i>S</i>	–	–	–
<i>Bo2g101910.1</i>	<i>R</i>	<i>S</i>	–	–	–
<i>Bo4g021310.1</i>	<i>R</i>	<i>S</i>	AT2G44150.1	ASHH3; Histone-lysine N-methyltransferase	–
<i>BnaA06g22180D</i>	<i>R</i>	<i>S</i>	–	–	–
<i>Bo7g077710.1</i>	<i>R</i>	<i>S</i>	AT5G47570.1	NADH dehydrogenase ubiquinone 1 beta subcomplex subunit	Dehydrogenase
<i>Cab031167.1</i>	<i>R</i>	<i>S</i>	–	–	–
<i>Cab017493.1</i>	<i>R</i>	<i>S</i>	AT5G56940.1	Ribosomal protein S16 family protein	Ribosomal protein
<i>Cab007887.1</i>	<i>S</i>	<i>R</i>	AT5G13310.1	–	–
<i>Bo6rg081580.1</i>	<i>S</i>	<i>R</i>	AT1G78420.2	DA2; Mono-ubiquitinitor	–
<i>Bo9g176310.1</i>	<i>S</i>	<i>R</i>	AT5G06310.1	POT1b; Protection of telomeres 1b	DNA metabolism protein
<i>Cab029870.1</i>	<i>S</i>	<i>R</i>	AT1G02560.1	CLPP5; Nuclear-encoded Clp protease 5	Serine protease
<i>Bo6rg081770.1</i>	<i>S</i>	<i>R</i>	AT1G78170.1	EAU1; Ethylene-responsive element binding factor-associated	–
<i>Cab032816.1</i>	<i>S</i>	<i>R</i>	AT1G24170.1	LGT9; Galacturonosyltransferase-like 8	Glycosyltransferase
<i>Cab027999.1</i>	<i>S</i>	<i>R</i>	–	–	–
<i>Cab018896.1</i>	<i>S</i>	<i>R</i>	AT1G76610.1	MIZU-KUSSEI-like protein	–
<i>Bo4g151450.1</i>	<i>S</i>	<i>R</i>	–	–	–
<i>Bo8g081460.1</i>	<i>S</i>	<i>R</i>	AT3G51570.1	Disease resistance protein (TIR-NBS-LRR class)	–
<i>Cab032851.1</i>	<i>S</i>	<i>R</i>	AT1G26630.1	FBR12; Fumonisin B1-resistant 12	Translation initiation factor
<i>Bo4g149580.1</i>	<i>S</i>	<i>R</i>	AT2G22400.1	TRM4B; S-adenosyl-L-methionine-dependent methyltransferases	RNA methyltransferase

Assessment of phenotypic variation segregating with alleles for Cab013526.1.135.A revealed that accessions inheriting a “G” at this locus had resistance values 57% lower than those inheriting an “A” (Fig. 3b). These alleles also segregated with resistance to *P. brassicae* (with “G” alleles showing 12% lower resistance than “A” alleles) and susceptibility to *A. brassicae* (with “G” alleles indicating 28% higher resistance than “A” alleles) (Fig. 3b). We calculated the distance in LD with this marker and found a region of 0.51 MB containing 107 genes (Fig. 3c).

Given the association between the expression of five nearby GEMs and *V. longisporum* resistance, we speculated that this link could partly be due to a genomic deletion in this region. To explore this, we examined whether any *B. napus* genotypes with published genomes (Quinta, Tapidor, Westar, and Zhongshuang 11) exhibited low gene expression and high susceptibility (Song et al. 2020). Quinta had little resistance to *V. longisporum* along with low expression of the five GEMs (expression at such levels could be a result of cross-mapping to the homologous region on the *B. napus* “C” genome, C08) (Fig. 3d). On the other hand, Tapidor, Westar, and Zhongshuang 11 exhibited moderate resistance and gene expression levels. We hypothesized that Quinta has

a deletion on *B. napus* chromosome A09, whereas Tapidor, Westar, and Zhongshuang 11 have not.

To determine the query coverage, defined as the percentage of the 0.51 MB region (comprising 107 genes in linkage disequilibrium with the most significant SNP marker) that aligned with the *B. napus* pan-transcriptome, we performed a BLAST analysis against the pan-transcriptome for each reference genotype. Among the 107 genes, a sequence of five consecutive genes displayed nearly 100% query coverage in Tapidor, Westar, and Zhongshuang 11, whereas Quinta exhibited reduced coverage: *Cab013522.1* (40%), *Cab013523.1* (0%), *Cab013524.1* (0%), *Cab013525.1* (0%), *Cab013526.1* (0%) (Table S8). BLAST analysis of the homologous region on chromosome C08 in Quinta revealed no differences compared to the other genotypes, suggesting a specific deletion on chromosome A09 (Fig. S2a). Linear regression analysis indicated that the expression of these five genes varied across *B. napus* genotypes and correlated with resistance to *V. longisporum* (Fig. S2b). This implies that both quantitative and qualitative resistance are associated with this region since both the deletion (qualitative) and gene expression in genotypes without the deletion (quantitative) correlate with resistance.

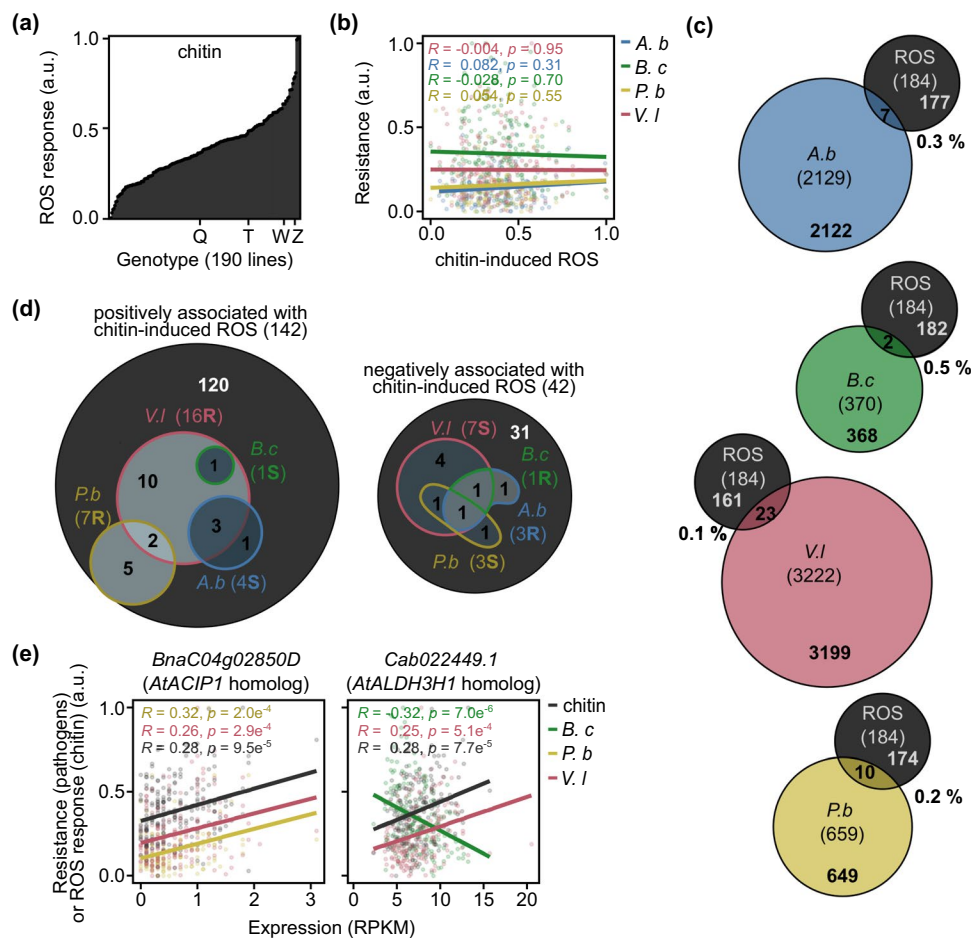


Fig. 2 Shared GEMs for QDR and chitin-induced ROS are associated with resistance to hemibiotrophic pathogens but susceptibility to necrotrophic pathogens. **a** Chitin-induced ROS response (arbitrary units (a.u.)) of the *B. napus* panel. Arbitrary units signify resistance values obtained through the reciprocal of disease susceptibility scores, derived from estimated marginal means and normalized to a 0–1 range for comparative data visualization. The positions of reference genotypes Quinta (Q), Tapidor (T), Westar (W), and Zhongshuang 11 (Z) are indicated. **b** Linear regression analysis of chitin-induced ROS response relative to quantitative disease resistance to *Alternaria brassicicola* (A.b), *Botrytis cinerea* (B.c), *Pyrenopeziza brassicae* (P.b), or *Verticillium longisporum* (V.l) (arbitrary units (a.u.)), normalized values between zero and one. **c** Venn diagrams

showing the overlap between GEMs associated with chitin-induced ROS and QDR to the fungal pathogens, *Alternaria brassicicola* (A.b), *Botrytis cinerea* (B.c), *Pyrenopeziza brassicae* (P.b), and *Verticillium longisporum* (V.l). The percentage of QDR-related GEMs which are also related to chitin-induced ROS is indicated. **d** The number of gene expression markers (GEMs) whose expression was positively or negatively associated with chitin-induced ROS and the number which was also associated with resistance (R) or susceptibility (S) to the *B. napus* fungal pathogens. Venn diagram indicating the overlap between GEMs associated with several pathogen interactions. **e** Linear regression analysis of gene expression (RPKM) of *BnaC04g02850D* and *Cab022449.1* relative to chitin-induced ROS responses and resistance to fungal pathogens

To identify potential genes within this deletion region that could contribute to *V. longisporum* resistance, we proposed that their homologs in the *B. napus* genome might also be relevant GEMs for resistance. Each of the five candidate genes on A09 only had one homolog, on chromosome C08. None of the five homologs were significant GEMs; however, linear regression analysis showed a significant association between gene expression of the *Cab013522.1* homolog (*Bo8g101810.1*) and the *Cab013524.1* homolog (*Bo8g101830.1*) and resistance to *V. longisporum* (Fig. S2b). Downstream of the five genes were two additional genes

with nearly 100% sequence coverage in Quinta but reduced coverage in Tapidor, Westar, and Zhongshuang 11: *BnaA09g43290D* (0%) and *Cab013532.1* (40%). However, neither of these genes was expressed during the third-leaf stage used for GEM analysis. The corresponding C08 homolog of *Cab013532.1* (*Bo8g101910.1*) also was not expressed at this stage, and no C08 homolog for *BnaA09g43290D* was identified.

To infer the potential function of the five gene candidates, we identified their putative *A. thaliana* orthologs using BLAST (Table 6). The orthologs included a

Table 5 The numbers of GEMs positively and negatively associated with chitin-induced ROS response and associated with either resistance (R) or susceptibility (S) to *Brassica napus* fungal pathogens. Fungal pathogens *Alternaria brassicicola*, *Botrytis cinerea*, *Pyr-*

enopeziza brassicae, or *Verticillium longisporum* are indicated. The direction of the correlation (positive or negative) of QDR GEMs compared to the chitin-induced ROS GEMs is also summarized

Pathogen	GEMs positively correlated with chitin-induced ROS (142)		GEMs negatively correlated with chitin-induced ROS (42)		Correlation to chitin-induced ROS GEMs
	Number	Type (R/S)	Number	Type (R/S)	
<i>A. brassicicola</i>	4	S	3	R	7 – ve
<i>B. cinerea</i>	1	S	1	R	2 – ve
<i>P. brassicae</i>	7	R	3	S	10 + ve
<i>V. longisporum</i>	16	R	7	S	23 + ve

microtubule-binding motor protein, *Kinesin motor family protein, KIN7.2 (Cab013522.1)*; a carbohydrate kinase, *Xylulose kinase 1, XK1 (Cab013523.1)*; a multidrug and toxin extrusion (MATE) transporter, *Enhanced disease susceptibility 5 homolog, EDS5H (Cab013524.1)*; a plastid isoform aldolase, *Fructose-bisphosphate aldolase 1, FBA1 (Cab013525.1)*; and a B-box zinc finger family transcription factor, *B-box domain protein 18, BBX18 (Cab013526.1)*.

Discussion

QDR is dependent on pathogen lifestyle

In this study, we used an AT pipeline to investigate constitutive QDR to *B. napus* fungal pathogens: *A. brassicicola*, *B. cinerea*, *P. brassicae*, and *V. longisporum* and define the “host genetic signature” of common and unique loci associated with resistance or susceptibility.

Throughout our analyses, we observed no significant GWA associations, in contrast to the discovery of numerous strongly significant associations through GEM analysis. While GWA primarily focuses on SNP variation, GEM explores how measurable variation in gene expression levels correlates with phenotypic traits. The limitation of GWA lies in its inability to capture the intricate complexity of gene regulation, interactions, and expression patterns, as it predominantly identifies genomic loci associated with traits without explicitly considering gene expression levels. Notably, SNP variation may or may not affect gene function, whereas gene expression often plays a direct role in determining the functional activity of genes. Moreover, variations such as SNPs and Indels in intergenic and promoter sequences, which have the potential to control gene expression, or variants within genes only induced following pathogen challenge, are not captured in mRNAseq and therefore will not be reflected in our GWA unless gene-based linked markers are present within the region. Additionally, high allelic heterogeneity may be

present across the association panel, reducing the ability to detect the effects of causal SNPs on phenotypes (Atwell et al. 2020). GEMs have been shown to be effective in identifying causal genes controlling glucosinolate content (Harper et al. 2012; Lu et al. 2014), seed erucic acid content (Havlickova et al. 2018), seed size, yield parameters, stem strength (Miller et al. 2018, 2019), flowering time (Woodhouse et al. 2021), and freezing stress (Huang et al. 2020). Our analyses further highlight the power of GEM in detecting the overarching molecular mechanisms that influence quantitative resistance traits.

We initially hypothesized broad-spectrum QDR across multiple pathogens with contrasting lifestyles. However, our findings revealed shared QDR loci only within similar pathogen lifestyles, either hemibiotrophic or necrotrophic. This distinction likely stems from differing infection strategies. In fact, phenotypic resistance to necrotrophic pathogens was inversely related to resistance against hemibiotrophic pathogens. This contrast was mirrored by 21 GEMs associated with broad-spectrum resistance or susceptibility to necrotrophic pathogens with an opposite association with hemibiotrophic pathogens.

Immune responses, such as cell death, can effectively counteract the endophytic growth of some pathogens like *P. brassicae* and *V. longisporum*, but necrotrophic pathogens like *A. brassicicola* and *B. cinerea* may exploit cell death mechanisms to promote their infection (McCombe et al. 2022). Such contrasting effects have been previously observed; for example, an NBS-LRR gene conferring resistance to biotrophic pathogen *Puccinia coronata* f. sp. *avenae* acts as a susceptibility factor (*LOV1*) for necrotrophic pathogen *Cochliobolus victoriae* (Lorang et al. 2007). Compellingly, in our study, the ortholog of a novel *A. thaliana* NBS-LRR, *Bo8g081460.1*, was associated with resistance to both hemibiotrophic pathogens and susceptibility to both necrotrophic pathogens, as was the predicted *A. thaliana* ortholog of *FBR12* which was previously shown to be involved in cell death induced by *Pseudomonas syringae* (Hopkins et al. 2008).

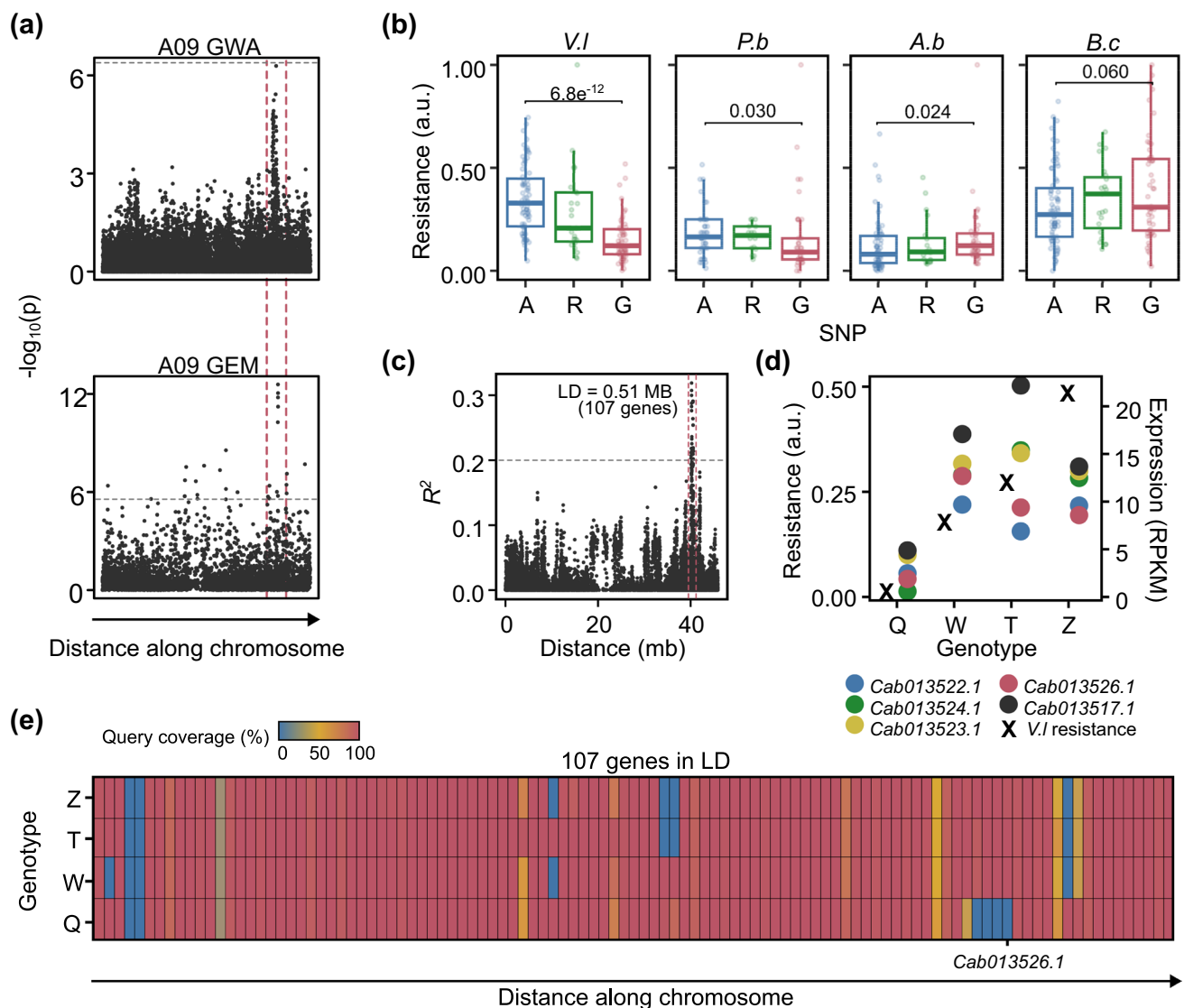


Fig. 3 Resistance to *Verticillium longisporum* is associated with a genomic deletion on chromosome A09. **a** Manhattan plots showing marker-trait association resulting from GEM and GWA analysis of resistance to *V. longisporum* in 193 *Brassica napus* genotypes. The x-axis indicates GEM or SNP location along the chromosome; the y-axis indicates the $-\log_{10}(p)$ (P value). Gray line indicates the FDR > 0.05 cut-off value, red line highlights the shared region. **b** Segregation of resistance to *V. longisporum* (*V.l*), *Pyrenopeziza brassicae* (*P.b*), *Alternaria brassicicola* (*A.b*), or *Botrytis cinerea* (*B.c*) (arbitrary units (a.u.)) with the highest associating marker, Cab013526.1.651.A, showing the marker effect between A and G ($R=A/G$). P values were determined by a Student's t test. Arbitrary units signify resistance values obtained through the reciprocal of dis-

ease susceptibility scores, derived from estimated marginal means and normalized to a 0–1 range for comparative data visualization. **c** Linkage decay plot from marker Cab013526.1.651.A as a function of genetic distance (MB). The gray line indicates an R^2 value of 0.2, red lines indicate the area of linkage disequilibrium. **d** Resistance to *V. longisporum* (left-hand y-axis) and gene expression (RPKM) of the five highest associating GEMs *Cab013522.1*, *Cab013524.1*, *Cab013523.1*, *Cab013526.1*, and *Cab013517.1* (right-hand y-axis) in reference genotypes Quinta (Q), Tapidor (T), Westar (W), and Zhongshuang 11 (Z). **e** Heatmap indicating query coverage (compared to the *B. napus* pan-transcriptome) in Q, T, W, and Z for the 107 genes predicted to be in linkage disequilibrium with Cab013526.1.651.A on chromosome A09

We explored the overlap between QDR loci and PTI and their varying associations with resistance based on pathogen lifestyle. While most QDR GEMs did not relate to PTI (Corwin et al. 2017), those that were positively associated with chitin-induced ROS response were associated with resistance to hemibiotrophic fungi but susceptibility to necrotrophic

fungi. For instance, the *B. napus* ortholog of *A. thaliana* *ALDH3H1* positively correlated with chitin-induced ROS response and *V. longisporum* resistance, yet negatively correlated with resistance to *B. cinerea*. ALDH proteins—for example, a homolog of *A. thaliana* *ALDH3H1*, *ALDH3I1*—can mitigate oxidative stress by scavenging ROS (Kotchoni

Table 6 The five genes in the deletion on chromosome A09 associated with resistance against *Verticillium longisporum*. The putative *Arabidopsis thaliana* (*At*) orthologs, gene ID, and protein class are indicated

GEM	<i>At</i> ortholog	Gene name	Protein class
<i>Cab013522.1</i>	<i>AT2G21380.1</i>	<i>KIN7.2</i> ; Kinesin motor family protein	Microtubule-binding motor protein
<i>Cab013523.1</i>	<i>AT2G21370.2</i>	<i>XK1</i> ; Xylulose kinase 1	Carbohydrate kinase
<i>Cab013524.1</i>	<i>AT2G21340.2</i>	<i>EDS5H</i> ; Enhanced disease susceptibility 5 homolog	Transporter (MATE efflux protein)
<i>Cab013525.1</i>	<i>AT2G21330.1</i>	<i>FBA1</i> ; Fructose-biphosphate aldolase 1	Aldolase
<i>Cab013526.1</i>	<i>AT2G21320.1</i>	<i>BBX18</i> ; B-box domain protein 18	Zinc family transcription factor

et al. 2006). Rapid ROS production during PTI can induce programmed cell death, which can confer susceptibility to necrotrophic pathogens like *B. cinerea* (Levine et al. 1994; Kotchoni and Gachomo 2006). *B. cinerea* even produces ROS to promote its infection (Govrin and Levine 2000), and ROS scavengers reduce infection severity (Tiedemann 1997). Thus, it follows that genotypes with a potentially greater ability to scavenge ROS would be less susceptible to *B. cinerea*.

It is intriguing that susceptibility to necrotrophic pathogens, resistance to hemibiotrophic pathogens, and ROS production aligned with a co-expressed module enriched in GEMs linked to photosynthesis regulation. Given that ROS are generated extensively during photosynthesis, it is reasonable to suggest that some genes influencing photosynthesis could impact ROS production levels, consequently influencing resistance to necrotrophic and hemibiotrophic pathogens. Indeed, previous studies have noted distinct regulation of photosynthesis-related genes during *A. brassicicola* infection (Macioszek et al. 2020).

Identification of a narrow chromosomal region associated with broad-spectrum QDR

By combining SNP and gene expression data through AT, we identified a novel locus associated with resistance to *V. longisporum*. Further in silico analyses of the region indicated five potential candidate genes, any of which could underlie the resistance phenotype. Alleles of the *BBX18* homolog also segregated with resistance to *P. brassicae*, and *KIN7.2*, *EDS5H*, and *BBX18* homologs were GEMs for resistance to *P. brassicae*, suggesting that these could be associated with broad-spectrum QDR. Although we investigated this region using reference genotype with a genomic deletion (qualitative resistance), the expression of the *KIN7.2*, *XK1*, *EDS5H*, *FBA1*, and *BBX18* homologs within other genotypes in the *B. napus* population varied and was significantly associated with resistance suggesting this locus is related to QDR.

KIN7.2 is involved in microtubule-based movement, and—in the animal field—kinesins have been implicated in protein trafficking for antifungal defense (Kurowska et al. 2012; Ogbomo et al. 2018). *EDS5H* is a homolog of *EDS5*,

encoding a MATE protein that functions in plant salicylic acid (SA) dependent defense (Nawrath et al. 2002). However, unlike *EDS5*, in *A. thaliana*, *EDS5H* is constitutively expressed in green tissues independent of pathogen infection and does not contribute to pathogen-induced SA accumulation (Parinthawong et al. 2015). Nevertheless, MATE proteins transport a broad range of substrates, such as organic acids, plant hormones, and secondary metabolites, which could influence QDR (Nawrath et al. 2002; Takanashi et al. 2014; Su et al. 2022). Conversely, *BBX18* and the additional *XK1* and *FBA1* genes in the potential deletion linked to resistance lack documented defense associations.

With our in silico analyses, we demonstrate the power of the AT pipeline to quickly narrow down on a predicted region of interest for broad-spectrum QDR. Additional functional analyses such as gene editing are needed to validate and identify the causal gene in *B. napus* and how it affects resistance to *V. longisporum* and other pathogens during infection.

Broad-spectrum QDR is an opportunity for crop breeding

Achieving broad-spectrum disease resistance without compromising resistance to other pathogens is a crucial goal in crop breeding. For example, GEMs associated with susceptibility and no antagonistic associations with resistance could be interesting targets for gene editing to improve disease control without the introduction of transgenes (Hua et al. 2019). In addition, considering crop breeding for resistance, we identified GEMs associated with resistance to both necrotrophic pathogens and no antagonistic associations with susceptibility to the hemibiotrophic pathogens. We also identified GEMs associated with resistance to both hemibiotrophic pathogens and no antagonistic associations with susceptibility to the necrotrophic pathogens including four GEMs homologous to *A. thaliana* *ACIP1*—*ACIP1* was previously implicated in flg22-induced ROS response and resistance to *Pseudomonas syringae* (Cheong et al. 2014). One of these four was positively associated with chitin-induced ROS response, highlighting it as a candidate for further investigation into its role in PTI and broad-spectrum

QDR. Future work could extend our findings to evaluate how broad the spectrum of disease control is likely to be using specific fungal strains or mutants, other *B. napus* pathogens, and different crop species.

Conclusions

Here, we used an AT pipeline to identify novel loci involved in QDR to several *B. napus* fungal pathogens *A. brassicicola*, *B. cinerea*, *P. brassicae*, and *V. longisporum*. We observed that broad-spectrum QDR loci were dependent on the lifestyle of the pathogen, as were associations with GEMs related to PAMP-induced ROS production. By combining GWA and GEM analyses, we were able to identify a novel region of interest for *V. longisporum* resistance and potentially broad-spectrum QDR. To our knowledge, this is the first time this approach with several pathosystems has been used to identify loci involved in broad-spectrum QDR. In summary, this study provides new insight into broad-spectrum QDR and highlights interesting targets for crop breeding.

Supplementary Information The online version contains supplementary material available at <https://doi.org/10.1007/s00122-024-04569-1>.

Author Contribution Statement VKM did experiments with *A. brassicicola* infection and analyzed the data with AKK. XZ did experiments and data curation with *V. longisporum* infection supervised by AvT. HF and GKM did experiments with *P. brassicae* and analyzed data with HUS and HF, and HUS and BDLF contributed to the conception and experimental design. RB and HJS did experiments and data curation with *B. cinerea* and PAMPs, HJS contributed to the conception and experimental design, and HJS and CNJ analyzed the data. CNJ did statistical analysis of all datasets, CNJ and RW did association transcriptomics, GSS did the WGCNA analysis, and BS did the BLAST validation of the genomic deletion. CNJ, RW, and CJR contributed to the conception, data interpretation, and in silico analyses post-AT. The first draft of the manuscript was written by CNJ, and all authors commented on subsequent versions of the manuscript. All authors read and approved the final manuscript.

Funding The authors thank Paweł Jedyński and Tomasz Jęcz (University of Lodz, Poland) for help with plant cultivation and inoculation with *A. brassicicola* and Aiming Qi for advice about *P. brassicae* data analysis. VKM and AKK were supported by the National Center for Research and Development, Poland (grant no. ERA-CAPS II/1/2015). XZ and AvT were supported by the German Research Foundation (grant no. ERA-CAPS DFG; TI170/13–1). HJS, RW, RB, CJR, HF, GKM, HUS, and BDLF were funded by the Biotechnology and Biological Sciences Research Council (BBSRC) grants BB/N005007/1 and BB/N005112/1 (as part of the ERA-CAPS consortium “MAQBAT”). HJS, RW, CNJ, GSS, RB, and CJR were also funded by the John Innes Institute strategic program grants Plant Health BB/P012574/1 (Response BBS/E/J/000PR9796), Molecules from Nature BB/P012523/1, Genes in the Environment BB/P013511/1, and Brassica Rapeseed and Vegetable Optimization (BRAVO) BB/P003095/1.

Data availability The R-based GAGA pipeline is available at <https://github.com/bsnichols/GAGA>. Our population structure is available in

Fell et al. (2023) [37]. Raw datasets used for the GAGA pipeline are available at Zenodo (<https://zenodo.org/records/10499917>). Inquiries related to the raw data can be directed to the respective scientific groups responsible for collecting the data and conducting preliminary analyses for each pathogen, as detailed in the author contributions section. Supplemental files are also available at <https://zenodo.org/record/8321694>.

Declarations

Conflict of interest The authors declare no competing interests.

Open Access This article is licensed under a Creative Commons Attribution 4.0 International License, which permits use, sharing, adaptation, distribution and reproduction in any medium or format, as long as you give appropriate credit to the original author(s) and the source, provide a link to the Creative Commons licence, and indicate if changes were made. The images or other third party material in this article are included in the article’s Creative Commons licence, unless indicated otherwise in a credit line to the material. If material is not included in the article’s Creative Commons licence and your intended use is not permitted by statutory regulation or exceeds the permitted use, you will need to obtain permission directly from the copyright holder. To view a copy of this licence, visit <http://creativecommons.org/licenses/by/4.0/>.

References

- Amas JC, Thomas WJ, Zhang Y, Edwards D, Batley J (2023) Key advances in the new era of genomics-assisted disease resistance improvement of *Brassica* species. *Phytopathology* 113(5):771–785. <https://doi.org/10.1094/PHYTO-08-22-0289-FI>
- Atwell S, Huang YS, Vilhjálmsson BJ, Willems G, Horton M, Li Y, Meng D, Platt A, Tarone AM, Hu TT, Jiang R (2020) Genome-wide association study of 107 phenotypes in *Arabidopsis thaliana* inbred lines. *Nature* 465(7298):627–631. <https://doi.org/10.1038/nature08800>
- Benson JM, Poland JA, Benson BM, Stromberg EL, Nelson RJ (2015) Resistance to gray leaf spot of maize: genetic architecture and mechanisms elucidated through nested association mapping and near-isogenic line analysis. *PLoS Genet* 11:e1005045. <https://doi.org/10.1371/journal.pgen.1005045>
- Bradbury PJ, Zhang Z, Kroon DE, Casstevens TM, Ramdoss Y, Buckler ES (2007) TASSEL: software for association mapping of complex traits in diverse samples. *Bioinformatics* 23:2633–2635. <https://doi.org/10.1093/bioinformatics/btm308>
- Brun H, Chèvre AM, Fitt BD, Powers S, Besnard AL, Ermel M, Huteau V, Marquer B, Eber F, Renard M, Andrivon D (2010) Quantitative resistance increases the durability of qualitative resistance to *Leptosphaeria maculans* in *Brassica napus*. *New Phytol* 185:285–299. <https://doi.org/10.1111/j.1469-8137.2009.03049.x>
- Cheong MS, Kirik A, Kim JG, Frame K, Kirik V, Mudgett MB (2014) AvrBsT acetylates *Arabidopsis* ACIP1, a protein that associates with microtubules and is required for immunity. *PLoS Pathog* 10:e1003952. <https://doi.org/10.1371/journal.ppat.1003952>
- Corwin JA, Kliebenstein DJ (2017) Quantitative resistance: more than just perception of a pathogen. *Plant Cell* 29:655–665. <https://doi.org/10.1105/tpc.16.00915>
- Corwin JA, Copeland D, Feusier J, Subedy A, Eshbaugh R, Palmer C, Maloof J, Kliebenstein DJ (2016) The quantitative basis of the *Arabidopsis* innate immune system to endemic pathogens depends on pathogen genetics. *PLoS Genet* 12:e1005789. <https://doi.org/10.1371/journal.pgen.1005789>
- Dakouri A, Lamara M, Karim M, Wang J, Chen Q, Gossen BD, Strelkov SE, Hwang S-F, Peng G, Yu F (2021) Identification

- of resistance loci against new pathotypes of *Plasmodiophora brassicae* in *Brassica napus* based on genome-wide association mapping. *Sci Rep* 11:6599. <https://doi.org/10.1038/s41598-021-85836-9>
- Deppe JP, Rabbat R, Hörtensteiner S, Keller B, Martinoia E, Lopéz-Marqués RL (2018) The wheat ABC transporter Lr34 modifies the lipid environment at the plasma membrane. *J Biol Chem* 293:18667–18679. <https://doi.org/10.1074/jbc.RA118.002532>
- Fell H, Ali AM, Wells R, Mitrousis GK, Woolfenden H, Schoonbeek H-J, Fitt BDL, Ridout CJ, Stotz H (2023) Novel gene loci associated with susceptibility or cryptic quantitative resistance to *Pyrenopeziza brassicae* in *Brassica napus*. *Theor Appl Genet* 136:71. <https://doi.org/10.1007/s00122-023-04243-y>
- Fisher MC, Hawkins NJ, Sanglard D, Gurr SJ (2018) Worldwide emergence of resistance to antifungal drugs challenges human health and food security. *Science* 360:739–742. <https://doi.org/10.1126/science.aap7999>
- Glazebrook J (2005) Contrasting mechanisms of defense against biotrophic and necrotrophic pathogens. *Annu Rev Phytopathol* 43:205–227. <https://doi.org/10.1146/annurev.phyto.43.040204.135923>
- Gómez-Gómez L, Boller T (2000) FLS2: an LRR receptor-like kinase involved in the perception of the bacterial elicitor flagellin in *Arabidopsis*. *Mol Cell* 5:1003–1011. [https://doi.org/10.1016/S1097-2765\(00\)80265-8](https://doi.org/10.1016/S1097-2765(00)80265-8)
- Govrin EM, Levine A (2000) The hypersensitive response facilitates plant infection by the necrotrophic pathogen *Botrytis cinerea*. *Curr Biol* 10:751–757. [https://doi.org/10.1016/S0960-9822\(00\)00560-1](https://doi.org/10.1016/S0960-9822(00)00560-1)
- Harper AL, Trick M, Higgins J, Fraser F, Clissold L, Wells R, Hattori C, Werner P, Bancroft I (2012) Associative transcriptomics of traits in the polyploid crop species *Brassica napus*. *Nat Biotechnol* 30:798–802. <https://doi.org/10.1038/nbt.2302>
- Havlickova L, He Z, Wang L, Langer S, Harper AL, Kaur H, Broadley MR, Gegas V, Bancroft I (2018) Validation of an updated associative transcriptomics platform for the polyploid crop species *Brassica napus* by dissection of the genetic architecture of erucic acid and tocopherol isoform variation in seeds. *Plant J* 93:181–192. <https://doi.org/10.1111/tpj.13767>
- He Z, Cheng F, Li Y, Wang X, Parkin IA, Chalhoub B, Liu S, Bancroft I (2015) Construction of Brassica A and C genome-based ordered pan-transcriptomes for use in rapeseed genomic research. *Data Brief* 4:357–362. <https://doi.org/10.1016/j.dib.2015.06.016>
- Hopkins MT, Lampi Y, Wang TW, Liu Z, Thompson JE (2008) Eukaryotic translation initiation factor 5A is involved in pathogen-induced cell death and development of disease symptoms in *Arabidopsis*. *Plant Physiol* 148:479–489. <https://doi.org/10.1104/pp.108.118869>
- Hua K, Zhang J, Botella JR, Ma C, Kong F, Liu B, Zhu J-K (2019) Perspectives on the application of genome-editing technologies in crop breeding. *Mol Plant* 12:1047–1059. <https://doi.org/10.1016/j.molp.2019.06.009>
- Huang M, Liu X, Zhou Y, Summers RM, Zhang Z (2019) BLINK: a package for the next level of genome-wide association studies with both individuals and markers in the millions. *Gigascience* 8:giy154. <https://doi.org/10.1093/gigascience/giy154>
- Huang Y, Hussain MA, Luo D, Xu H, Zeng C, Havlickova L, Bancroft I, Tian Z, Zhang X, Cheng Y, Zou X (2020) A *Brassica napus* reductase gene dissected by associative transcriptomics enhances plant adaptation to freezing stress. *Front Plant Sci* 26(11):971. <https://doi.org/10.3389/fpls.2020.00971>
- Hurni S, Scheuermann D, Krattinger SG, Kessel B, Wicker T, Herren G, Fitze MN, Breen J, Presterl T, Ouzunova M (2015) The maize disease resistance gene *Htn1* against northern corn leaf blight encodes a wall-associated receptor-like kinase. *Proc Natl Acad Sci* 112:8780–8785. <https://doi.org/10.1073/pnas.1502522112>
- Jia Y, McAdams SA, Bryan GT, Hershey HP, Valent B (2000) Direct interaction of resistance gene and avirulence gene products confers rice blast resistance. *EMBO J* 19:4004–4014. <https://doi.org/10.1093/emboj/19.15.4004>
- Kemen E, Jones JDG (2012) Obligate biotroph parasitism: can we link genomes to lifestyles? *Trends Plant Sci* 17:448–457. <https://doi.org/10.1016/j.tplants.2012.04.005>
- Kim S, Kiraly M, Jiang M, Stuart JM, Eizinger Am Wylie BN, Davidson GS (2001) A gene expression map for *Caenorhabditis elegans*. *Science* 5537:2087–2092. <https://doi.org/10.1126/science.1061603>
- Kotchoni SO, Gachomo EW (2006) The reactive oxygen species network pathways: an essential prerequisite for perception of pathogen attack and the acquired disease resistance in plants. *J Biosci* 31:389–404. <https://doi.org/10.1007/bf02704112>
- Kotchoni SO, Kuhns C, Ditzer A, Kirch HH, Bartels D (2006) Overexpression of different *aldehyde dehydrogenase* genes in *Arabidopsis thaliana* confers tolerance to abiotic stress and protects plants against lipid peroxidation and oxidative stress. *Plant, Cell Environ* 29:1033–1048. <https://doi.org/10.1111/j.1365-3040.2005.01458.x>
- Kou Y, Wang S (2010) Broad-spectrum and durability: understanding of quantitative disease resistance. *Curr Opin Plant Biol* 13:181–185. <https://doi.org/10.1016/j.pbi.2009.12.010>
- Kurowska M, Goudin N, Nehme NT, Court M, Garin J, Fischer A, de Saint BG, Ménasché G (2012) Terminal transport of lytic granules to the immune synapse is mediated by the kinesin-1/Slp3/Rab27a complex. *Blood* 119:3879–3889. <https://doi.org/10.1182/blood-2011-09-382556>
- Lacombe S, Rougon-Cardoso A, Sherwood E, Peeters N, Dahlbeck D, van Esse HP, Smoker M, Rallapalli G, Thomma BP, Staskawicz B et al (2010) Interfamily transfer of a plant pattern-recognition receptor confers broad-spectrum bacterial resistance. *Nat Biotechnol* 28:365–369. [https://doi.org/10.1016/0006-291x\(75\)90482-9](https://doi.org/10.1016/0006-291x(75)90482-9)
- Langfelder P, Horvath S (2008) WGCNA: an R package for weighted correlation network analysis. *BMC Bioinformatics* 9:559. <https://doi.org/10.1186/1471-2105-9-559>
- Levine A, Tenhaken R, Dixon R, Lamb C (1994) H₂O₂ from the oxidative burst orchestrates the plant hypersensitive disease resistance response. *Cell* 79:583–593. [https://doi.org/10.1016/0092-8674\(94\)90544-4](https://doi.org/10.1016/0092-8674(94)90544-4)
- Lipka AE, Tian F, Wang Q, Peiffer J, Li M, Bradbury PJ, Gore MA, Buckler ES, Zhang Z (2012) GAPIT: genome association and prediction integrated tool. *Bioinformatics* 28:2397–2399. <https://doi.org/10.1093/bioinformatics/bts444>
- Liu X, Huang M, Fan B, Buckler ES, Zhang Z (2016) Iterative usage of fixed and random effect models for powerful and efficient genome-wide association studies. *PLoS Genet* 12:e1005767. <https://doi.org/10.1371/journal.pgen.1005767>
- Lloyd SR, Schoonbeek H-J, Trick M, Zipfel C, Ridout CJ (2014) Methods to study PAMP-triggered immunity in *Brassica* species. *Mol Plant Microb Interact* 27:286–295. <https://doi.org/10.1094/mpmi-05-13-0154-fi>
- Lorang JM, Sweat TA, Wolpert TJ (2007) Plant disease susceptibility conferred by a “resistance” gene. *Proc Natl Acad Sci* 104:14861–14866. <https://doi.org/10.1073/pnas.0702572104>
- Lu G, Harper AL, Trick M, Morgan C, Fraser F, O’Neill C, Bancroft I (2014) Associative transcriptomics study dissects the genetic architecture of seed glucosinolate content in *Brassica napus*. *DNA Res* 21(6):613–625. <https://doi.org/10.1093/dnares/dsu024>
- Macioszek VK, Lawrence CB, Kononowicz AK (2018) Infection cycle of *Alternaria brassicicola* on *Brassica oleracea* leaves under growth room conditions. *Plant Pathol* 67:1088–1096. <https://doi.org/10.1111/ppa.12828>
- Macioszek VK, Gapińska M, Zmienko A, Sobczak M, Skoczowski A, Oliwa J, Kononowicz AK (2020) Complexity of *Brassica*

- oleracea*–*Alternaria brassicicola* susceptible interaction reveals downregulation of photosynthesis at ultrastructural, transcriptional, and physiological levels. *Cells* 9:2329. <https://doi.org/10.3390/cells9102329>
- McCombe CL, Greenwood JR, Solomon PS, Williams SJ (2022) Molecular plant immunity against biotrophic, hemibiotrophic, and necrotrophic fungi. *Essays Biochem* 66:581–593. <https://doi.org/10.1042/ebc20210073>
- McDowell JM, Woffenden BJ (2003) Plant disease resistance genes: recent insights and potential applications. *Trends Biotechnol* 21:178–183. [https://doi.org/10.1016/s0167-7799\(03\)00053-2](https://doi.org/10.1016/s0167-7799(03)00053-2)
- Miller CN, Harper AL, Trick M, Wellner N, Werner P, Waldron KW, Bancroft I (2018) Dissecting the complex regulation of lodging resistance in *Brassica napus*. *Mol Breeding* 38:1–18. <https://doi.org/10.1007/s11032-018-0781-6>
- Miller C, Wells R, McKenzie N, Trick M, Ball J, Fatihi A, Dubreucq B, Chardot T, Lepiniec L, Bevan MW (2019) Variation in expression of the HECT E3 ligase UPL3 modulates LEC2 levels, seed size, and crop yields in *Brassica napus*. *Plant Cell* 31(10):2370–2385. <https://doi.org/10.1105/tpc.18.00577>
- Miya A, Albert P, Shinya T, Desaki Y, Ichimura K, Shirasu K, Narusaka Y, Kawakami N, Kaku H, Shibuya N (2007) CERK1, a LysM receptor kinase, is essential for chitin elicitor signaling in *Arabidopsis*. *Proc Natl Acad Sci* 104:19613–19618. <https://doi.org/10.1073/pnas.0705147104>
- Moore JW, Herrera-Foessel S, Lan C, Schnippenkoetter W, Ayliffe M, Huerta-Espino J, Lillemo M, Viccars L, Milne R, Periyannan S (2015) A recently evolved hexose transporter variant confers resistance to multiple pathogens in wheat. *Nat Genet* 47:1494–1498. <https://doi.org/10.1038/ng.3439>
- Navarro L, Bari R, Achard P, Lisón P, Nemri A, Harberd N, Jones J (2008) DELLAs control plant immune responses by modulating the balance of jasmonic acid and salicylic acid signaling. *Curr Biol* 18:650–655. <https://doi.org/10.1016/j.cub.2008.03.060>
- Nawrath C, Heck S, Parinthewong N, Métraux J-P (2002) EDS5, an essential component of salicylic acid-dependent signaling for disease resistance in *Arabidopsis*, is a member of the MATE transporter family. *Plant Cell* 14:275–286. <https://doi.org/10.1105/tpc.010376>
- Nelson R, Wiesner-Hanks T, Wissner R, Balint-Kurti P (2018) Navigating complexity to breed disease-resistant crops. *Nat Rev Genet* 19:21–33. <https://doi.org/10.1038/nrg.2017.82>
- Nichols B (2022) A pipeline for GEM And GWAS automation. *GitHub* URL <https://github.com/bsnichols/GAGA>. <https://zenodo.org/badge/latestdoi/512807075>
- Ogbomo H, Timm-McCann M, Barnes T, Xiang RF, Jamil K, Ganguly A, Stack D, Huston SM, Li SS, Colarusso P (2018) Granule-dependent NK cell killing of cryptococcus requires kinesin to reposition the cytolytic machinery for directed cytotoxicity. *Cell Rep* 24:3017–3032. <https://doi.org/10.1016/j.celrep.2018.08.027>
- Parinthewong N, Cottier S, Buchala A, Nawrath C, Métraux J-P (2015) Localization and expression of EDS5H a homologue of the SA transporter EDS5. *BMC Plant Biol* 15:135. <https://doi.org/10.1186/s12870-015-0518-1>
- Pilet-Nayel ML, Moury B, Caffier V, Montarry J, Kerlan MC, Fournet S, Durel CE, Delourme R (2017) Quantitative resistance to plant pathogens in pyramiding strategies for durable crop protection. *Front Plant Sci* 8:1838. <https://doi.org/10.3389/fpls.2017.01838>
- Plaisier SB, Taschereau R, Wong JA, Graeber TG (2010) Rank–rank hypergeometric overlap: identification of statistically significant overlap between gene-expression signatures. *Nucleic Acids Res* 38:e169. <https://doi.org/10.1093/nar/gkq636>
- Qasim MU, Zhao Q, Shahid M, Samad RA, Ahmar S, Wu J, Fan C, Zhou Y (2020) Identification of QTLs containing resistance genes for Sclerotinia stem rot in *Brassica napus* using comparative transcriptomic studies. *Front Plant Sci* 11:776. <https://doi.org/10.3389/fpls.2020.00776>
- R Core Team (2023). R: A Language and Environment for Statistical Computing. R Foundation for Statistical Computing, Vienna, Austria.
- Raman R, Diffey S, Barbulescu DM, Coombes N, Luckett D, Salisbury P, Cowley R, Marcroft S, Raman H (2020) Genetic and physical mapping of loci for resistance to blackleg disease in canola (*Brassica napus* L.). *Sci Rep* 10:4416. <https://doi.org/10.1038/s41598-020-61211-y>
- Roux F, Voisin D, Badet T, Balagué C, Barlet X, Huard-Chauveau C, Roby D, Raffaele S (2014) Resistance to phytopathogens *e tutti quanti*: placing plant quantitative disease resistance on the map. *Mol Plant Pathol* 15:427–432. <https://doi.org/10.1111/mpp.12138>
- Roy J, Shaikh TM, del Río ML, Hosain S, Chapara V, Rahman M (2021) Genome-wide association mapping and genomic prediction for adult stage sclerotinia stem rot resistance in *Brassica napus* (L.) under field environments. *Sci Rep* 11:21773. <https://doi.org/10.1038/s41598-021-01272-9>
- Samira R, Kimball JA, Samayoa LF, Holland JB, Jamann TM, Brown PJ, Stacey G, Balint-Kurti PJ (2020) Genome-wide association analysis of the strength of the MAMP-elicited defense response and resistance to target leaf spot in sorghum. *Sci Rep* 10:20817. <https://doi.org/10.1038/s41598-020-77684-w>
- Schoonbeek H-J, Del Sorbo G, De Waard MA (2001) The ABC transporter BcatrB affects the sensitivity of *Botrytis cinerea* to the phytoalexin resveratrol and the fungicide fenpiclonil. *Mol Plant Microbe Interact* 14:562–571. <https://doi.org/10.1094/mpmi.2001.14.4.562>
- Schoonbeek H-J, Wang HH, Stefanato FL, Craze M, Bowden S, Wallington E, Zipfel C, Ridout CJ (2015) Arabidopsis EF-Tu receptor enhances bacterial disease resistance in transgenic wheat. *New Phytol* 206:606–613. <https://doi.org/10.1111/nph.13356>
- Schweizer P, Stein N (2011) Large-scale data integration reveals colocalization of gene functional groups with meta-QTL for multiple disease resistance in barley. *Mol Plant Microbe Interact* 24:1492–1501. <https://doi.org/10.1094/mpmi-05-11-0107>
- Song J-M, Guan Z, Hu J, Guo C, Yang Z, Wang S, Liu D, Wang B, Lu S, Zhou R (2020) Eight high-quality genomes reveal pan-genome architecture and ecotype differentiation of *Brassica napus*. *Nature Plants* 6:34–45. <https://doi.org/10.1038/s41477-019-0577-7>
- Stefanato FL, Abou-Mansour E, Buchala A, Kretschmer M, Mosbach A, Hahn M, Bochet CG, Métraux JP, Schoonbeek H-J (2009) The ABC transporter BcatrB from *Botrytis cinerea* exports camalexin and is a virulence factor on *Arabidopsis thaliana*. *Plant J* 58:499–510. <https://doi.org/10.1111/j.1365-3113X.2009.03794.x>
- Storey JD (2011) False discovery rate. In: Lovric M (ed) *International encyclopedia of statistical science*. Springer, Heidelberg, Berlin, Germany, pp 504–508
- Su Q, Rong W, Zhang Z (2022) The pathogen-induced MATE gene *TaP1MA1* is required for defense responses to *Rhizoctonia cerealis* in wheat. *Int J Mol Sci* 23:3377. <https://doi.org/10.3390/ijms23063377>
- Takanashi K, Shitan N, Yazaki K (2014) The multidrug and toxic compound extrusion (MATE) family in plants. *Plant Biotechnol* 31:417–430. <https://doi.org/10.5511/plantbiotechnology.14.0904a>
- Tiedemann AV (1997) Evidence for a primary role of active oxygen species in induction of host cell death during infection of bean leaves with *Botrytis cinerea*. *Physiol Mol Plant Pathol* 50:151–166. <https://doi.org/10.1006/pmpp.1996.0076>
- Vetter MM, Kronholm I, He F, Häweker H, Reymond M, Bergelson J, Robatzek S, de Meaux J (2012) Flagellin perception varies quantitatively in *Arabidopsis thaliana* and its relatives. *Mol Biol Evol* 29:1655–1667. <https://doi.org/10.1093/molbev/mss011>
- Vleeshouwers VGAA, van Dooijeweert W, Govers F, Kamoun S, Colon LT (2000) The hypersensitive response is associated with host and

- nonhost resistance to *Phytophthora infestans*. *Planta* 210:853–864. <https://doi.org/10.1007/s004250050690>
- Wang J, Zhang Z (2021) GAPIT Version 3: boosting power and accuracy for genomic association and prediction. *Genom Proteomics Bioinform* 19:629–640. <https://doi.org/10.1016/j.gpb.2021.08.005>
- Wisser RJ, Sun Q, Hulbert SH, Kresovich S, Nelson RJ (2005) Identification and characterization of regions of the rice genome associated with broad-spectrum, quantitative disease resistance. *Genetics* 169:2277–2293. <https://doi.org/10.1534/genetics.104.036327>
- Woodhouse S, He Z, Woolfenden H, Steuernagel B, Haerty W, Bancroft I, Irwin JA, Morris RJ, Wells R (2021) Validation of a novel associative transcriptomics pipeline in *Brassica oleracea*: identifying candidates for vernalisation response. *BMC Genom* 22:1–13. <https://doi.org/10.1186/s12864-021-07805-w>
- Zeise K, Tiedemann AV (2001) Morphological and physiological differentiation among vegetative compatibility groups of *Verticillium dahliae* in relation to *V. longisporum*. *J Phytopathol* 149:469–475. <https://doi.org/10.1111/j.1439-0434.2001.tb03879.x>
- Zheng X, Koopmann B, von Tiedemann A (2019) Role of salicylic acid and components of the phenylpropanoid pathway in basal and cultivar-related resistance of oilseed rape (*Brassica napus*) to *Verticillium longisporum*. *Plants* 8:491. <https://doi.org/10.3390/plants8110491>
- Zheng X (2018) *Verticillium longisporum* on oilseed rape (*Brassica napus* L.): differential roles of salicylic acid, seed transmission and plant colonization in greenhouse and field conditions. Dissertation, Niedersächsische Staats-und Universitätsbibliothek Göttingen, Germany
- Zipfel C, Kunze G, Chinchilla D, Caniard A, Jones JD, Boller T, Felix G (2006) Perception of the bacterial PAMP EF-Tu by the receptor EFR restricts *Agrobacterium*-mediated transformation. *Cell* 125:749–760. <https://doi.org/10.1016/j.cell.2006.03.037>

Publisher's Note Springer Nature remains neutral with regard to jurisdictional claims in published maps and institutional affiliations.